Operational model evaluation for particulate matter in Europe and North America in the context of the AQMEII project

Efisio Solazzo[1,] ,Roberto Bianconi[2],Guido Pirovano[6,7], Volker Matthias [17], Robert Vautard[3], K. Wyat Appel[9], Bertrand Bessagnet[6], Jørgen Brandt[16], Jesper H. Christensen[16], Charles Chemel[11,12], Isabelle Coll[15], Joana Ferreira[8], Renate Forkel[10], Xavier V. Francis[12], George Grell[18], Paola Grossi[2], Ayoe Hansen[16], Ana Isabel Miranda[8], Michael D. Moran[14], Uarporn Nopmongcol[4], Marje Parnk[19], Karine N. Sartelet[5], Martijn Schaap[20], Jeremy D. Silver[16], Ranjeet S. Sokhi[12], Julius Vira[19], Johannes Werhahn[10], Ralf Wolke[13], Gregg Yarwood[4], Junhua Zhang[14], S.Trivikrama Rao[9], Stefano Galmarini[1, *]

[1]Joint Research Centre, European Commission, ISPRA, Italy;

[2]Enviroware srl, via Dante 142, 20863 Concorezzo (MB), Italy

[3]IPSL/LSCE Laboratoire CEA/CNRS/UVSQ

[4]Environ International Corporation, Novato CA, USA

[5]CEREA, Joint Laboratory Ecole des Ponts ParisTech/ EDF R & D, Université Paris-Est, France

[6]Ineris, Parc Technologique Halatte, France

[7] Ricerca sistema energetico (RSE), Italy

[8]CESAM & Department of Environment and Planning, University of Aveiro, Aveiro, Portugal

[9]Atmospheric Modelling and Analysis Division, Environmental Protection Agency, NC, USA

[10]IMK-IFU, Institute for Meteorology and Climate Research-Atmospheric Environmental Division, Germany

[11]National Centre for Atmospheric Science (NCAS), University of Hertfordshire, Hatfield, UK

[12] Centre for Atmospheric & Instrumentation Research (CAIR), University of Hertfordshire, Hatfield, UK

[13] Leibniz Institute for Tropospheric Research, Leipzig, Germany

[14]Air Quality Research Division, Science and Technology Branch, Environment Canada, Toronto, Canada

[15] IPSL/LISA UMR CNRS 7583, Université Paris Est Créteil et Université Paris Diderot

[16]Department of Atmospheric Environment, National Environmental Research Institute, Aarhus University, Denmark

[17] Institute of Coastal Research, Helmholtz-Zentrum Geesthacht,Geeshacht, Germany

[18]CIRES-NOAA/ESRL/GSD National Oceanic and Atmospheric Administration Environmental Systems Research Laboratory Global Systems Division Boulder, Colorado USA

[19]Finnish Meteorological Institute, Helsinki, Finland

[20]Netherlands Organization for Applied Scientific Research (TNO), Utrecht, The Netherlands

---

[*] Author for correspondence: S.Galmarini. Email: Stafano.Galmarini@jrc.europa.eu

Abstract. More than ten state-of-the-art regional air quality models have participated in the Air Quality Model Evaluation International Initiative (AQMEII), in which a variety of mesoscale air quality modeling systems have been applied to continental-scale domains in North America and Europe for 2006 full-year simulations. The main goal of AQMEII is model inter-comparisons and evaluations. Standardised modelling outputs from each group have been shared on the web distributed ENSEMBLE system, which allows statistical and ensemble analyses to be performed. In this study, the simulations issued from the models are inter-compared and evaluated with a large set of observations for ground level aerosol (PM_{10} and $PM_{2.5}$) and its components, in both the continents. To facilitate the discussion and interpretation of the results, three sub-regions for each continental domain have been selected and analyses, with focus on spatially-averaged concentration. The unprecedented scale of the exercise (two continents, one year, over twenty groups) allows for a detailed description of model's skill and uncertainty.

Analysis of PM_{10} yearly time series and daily cycles indicates that large positive biases exist for all the investigated region and time of the year. We seek possible causes of PM bias in the emission and deposition balance, and in the bias induced by meteorological factors, such as the wind speed. $PM_{2.5}$ and its major components are then analysed, and model performances highlighted. Finally, capability of models to capture high PM concentrations is also evaluated by looking at two separate $PM_{2.5}$ episodes in Europe and North America.

In particular, we found a large variability among models in predicting emissions, deposition, and PM concentration (especially PM_{10}). Major challenges still remain to eliminate the sources of PM bias. Although $PM_{2.5}$ is, by far, better estimated than PM_{10}, no model was found to consistently match the observations under of variety of scenarios (sub-region and time of the year).

1. Introduction

Particulate matter (PM) is a worldwide environmental concern as it threatens human health and ecosystems (Manders et al., 2009; Aan de Brugh et al., 2011). Human exposure to high PM concentrations is associated with respiratory disease and shortened life expectancy (Amann et al., 2005; Cohen et al., 2005). PM also contributes to acid rain, visibility degradation, and modification of the Earth surface energy balance, and thus contributes to short-term climate forcings (Forster, 2007; Mebust et al., 2003; Appel et al., 2008; Smyth et al., 2009; Boylan et al., 2006 Wild et al.,

2009). Recent studies have suggested that long-term changes in aerosol concentrations, especially due to decreasing use of coal for energy production, have significantly influenced regional warming rates (Vautard et al., 2009; Philipona et al., 2009; Yiou et al., 2011). Although major efforts are being made to reduce anthropogenic emissions of primary PM and aerosol precursors, PM levels remain problematic and their adverse effects are foreseen to persist (Klimont et al., 2009). The characterisation of PM sources is an area of active research, as many gaps in the knowledge of the chemical speciation of sources, spatial and temporal distribution of airborne particles, physical and chemical transformation, need to be filled. This is particularly true for atmospheric chemistry transport models (CTMs), for which incorporating the wide range of PM physics and chemistry, as well as dealing with the large variety of PM sources is very challenging, especially when simulating on long temporal and large spatial scales.

PM is a conglomerate of many different types of particles (i.e. elemental and organic carbon, ammonium, nitrates, sulphates, mineral dust, trace elements, water) with varying physical and chemical properties. Particles are either emitted directly from a large number of sources and source types or formed from a variety of chemical/physical transformation of other species, which depend, among other factors, on their size. Furthermore, given its composite nature, high PM concentrations might be observed at any time during the year and under a large variety of atmospheric conditions (unlike, for example, ozone which is typically associated with hot and stagnant conditions). A widely accepted classification of PM is based on the size of particles: those with diameter between 2.5 and 10 μm are referred to as coarse particles (PM_{10}), while particles less than 2.5 μm in diameter ($PM_{2.5}$) are referred to as fine particles. PM_{10} and $PM_{2.5}$ is a widely accepted nomenclature to define particles with diameter less than 10 and 2.5 μm, respectively (note that PM_{10} includes $PM_{2.5}$). This classification is dictated by the fact that the mechanisms for the generation, transformation, removal and deposition, chemical composition and optical properties of the two classes of particles are notably different. The particles also behave differently in the human respiratory track, with the fine fractions penetrating deeper (see, e.g., Seinfeld and Pandis (2006) for a detailed description of particles properties). In the last decade, the fine particles have attracted much more attention than coarse particles due to their adverse effect on public health. As a result, air quality models have developed strong skills in modelling $PM_{2.5}$, made possible by the availability of comprehensive $PM_{2.5}$ measurements which allows model performance to be evaluated for the individual PM chemical components, which, in turn, allows deductions about different aspects of model performance (e.g., the relationships between emissions, dispersion, chemistry and deposition) (refs).

Given the large impact of PM on public health and climate, accurate predictions and assessments are required. CTMs are routinely used for assessing and forecasting PM concentrations. Reliable global and regional modelling systems are therefore highly beneficial. The analysis presented in this paper focuses on model cross-comparison (model to model comparison) and model evaluation (model to observation comparison), with models sharing common emission inventories and chemistry boundary conditions. Such an approach is of direct relevance for model evaluation, and is the focus of the Air Quality Model Evaluation International Initiative (AQMEII) (Rao et al., 2011), an international project aimed at joining the knowledge and the experiences of modelling groups in Europe and North America. Within AQMEII, standardised modelling outputs have been shared on the web distributed ENSEMBLE system, which allows statistical and ensemble analyses to be performed (Bianconi et al., 2004). A common exercise was launched for modelling communities to use their CTMs to retrospectively simulate the whole year 2006, for the two continents of Europe and North America. Outputs of regional air quality models have been submitted in the form of hourly average concentrations on a grid of points and at specific locations, allowing direct comparison with air quality measurements collected from monitoring networks, for model evaluation (details are given in Rao et al. (2011) and can be found at http://aqmeii.jrc.ec.europa.eu/aqmeii2.htm). The primary goal of AQMEII is, in fact, to test the ability of CTMs to reconstruct atmospheric pollutants concentrations and not to forecast air quality. This type of evaluation, with large temporal and spatial coverage, is essential for determining model performance and assessing model deficiencies (Rao et al., 2011; Dennis et al., 2010).

Although previous attempts of model harmonisation for PM have been undertaken (Smyth et al., 2009; van Loon et al., 2007; Stern et al., 2008; Vautard et al., 2009; Hayami et al. 2008), the unprecedented effort of the AQMEII community to provide a comprehensive set of model's variables for two continents and for an entire year, offers a unique opportunity for model cross-comparison and evaluation. In this paper we focus on the evaluation of the performance of ensemble modelling for PM in Europe and North America, for which over ten state-of-the-art regional air quality models, run by twenty independent groups from both continents, have submitted their results and for which observational data are made available on the ENSEMBLE system (described in Section 2). Emphasis of the analyses is dedicated to PM_{10} and $PM_{2.5}$. In particular, the analysis of PM_{10} is presented in Sections 3, and it is mostly devoted to study the possible sources responsible for model bias. Investigation of $PM_{2.5}$ focuses on the chemical compositions and models performance, discussed in Section 4. An analysis of two episodes with elevated PM2.5

levels, one for each continent, is also presented (Section 5). Main conclusions are drawn in Section

140 6.

2. Monitoring data and participating models

2.1 Data used for analysis within AQMEII

145 In order to carry out an exhaustive evaluation of regional air quality models across seasons, models are compared to observations over the full year of 2006. Modelling groups provided gridded surface daily concentration of PM_{10}, $PM_{2.5}$ and other compounds (such as hourly SO_2 and NO_2), covering the area (15°W - 35°E; 35°N - 70°N) for EU and the area (130°W – 58.5°W; 23.5°N – 59.5°N) for NA. Additional to the gridded surface concentrations, modellers were required to provide hourly

150 averaged surface concentrations of the same species and at the same sites where observations at receptors are available. Moreover, at several receptors positions in NA, speciated $PM_{2.5}$ data are also accessible. The analyses presented in this paper are derived by comparing the model results with PM measurements routinely taken at receptors sites. In order to fully explore each model's capability, AQMEII participants also provided modelled emission and deposition data for several

155 species, allowing an exhaustive model cross-comparison to be carried out.

2.2 Participating models

Table 1 summarises the CTMs that have been used in the AQMEII activity, to provide PM concentrations at receptor sites for the European (EU) and North American (NA) domains. These

160 are:

- CHIMERE (Bessagnet et al., 2004);
- POLYPHEMUS (Sartelet et al., 2007; Mallet et al., 2007);
- CAMx (Environ., 2010);
- COSMO-MUSCAT (Multi Scale Chemistry Aerosol Model) (Wolke et al., 2004; Renner

165 and Wolke, 2010);
- SILAM (Sofiev et al., 2006);
- DEHM (Brandt et al., 2007);
- CMAQ (Foley et al., 2010);
- LOTOS-EUROS (Long term Ozone simulation-European Operational Smog Model)

170 (Schaap et al., 2008);
- AURAMS (Gong et al., 2006; Smyth et al., 2009)

The CHIMERE, CAMx, CMAQ and DEHM models have been applied over both continents, while the POLYPHEMUS, COSMO-MUSCAT, SILAM, and LOTOS-EUROS models were applied for

the EU only. AURAMS was the only model which was run exclusively over NA. Meteorological drivers for these models are also listed in Table 1. Most of the simulations for EU (CHIMERE, POLYPHEMUS, CAMx, DEHM) used meteorological fields generated by different versions of the 5th Generation Mesoscale Model (MM5; Dudhia, 1993). The SILAM and LOTOS-EUROS models used meteorological data provided by the European Centre for Medium-range Weather Forecasting (ECMWF), while the WRF v3.1 (Skamarock et al., 2008) meteorological model was used to provide meteorological input data for the CMAQ model over EU and NA (run by two different groups), and for the CHIMERE model over NA only. The MUSCAT model used meteorological data provided by the German COSMO-CLM model. Finally, meteorology from the GEM model was used for running AURAMS over NA. A more detailed description and assessment of the model performance for the various meteorological models used can be found in Vautard et al. (this issue, in prerparation).

The CTMs used in the current analysis take very different approaches in estimating PM concentrations. The key physical and chemical mechanisms are handled in different ways by the models. Several aspects of models settings are summarised in Table 1. The number of bins for particle sizes varies between one (LOTOS-EUROS) and eight (CHIMERE), with the majority of models having two size bins (PM_{10} and $PM_{2.5}$). The ISORROPIA (Nenes et al., 1998) module is predominantly used to perform the thermodynamic equilibrium within the CTMS. The dry deposition mechanisms are modelled using the resistance analogy described by Seinfeld and Pandis (2006), whereas the wet deposition is modelled by various modification of the scavenging approach. Full details are given in Table 1 and references therein. Horizontal and vertical resolutions were not harmonised within AQMEII, thus participants applied their own settings. Table 1 reports the number of vertical layers used for each model, ranging from 34 layers in the CMAQ simulations to only four for LOTOS-EUROS model simulation (adjusting their position to the height of the boundary layer). The majority of the model simulations use between nine and more than twenty (three models each) layers, with a greater number of layers in the lower portion of the troposphere.

Concerning emissions, it should be noted that AQMEII participants were given the opportunity to use a set of "standard" emissions and boundary conditions for each continent. The EU "standard" emissions were prepared by TNO, which provided a gridded emissions database for the year 2005 and 2006. The provided EU emissions dataset is widely used, for instance within the GEMS project (http://gems.ecmwf.int). The dataset consists of European anthropogenic emissions for the 10

6

SNAP sectors and international shipping on a 0.125 by 0.0625 degree lon-lat resolution. Biomass burning emissions were provided by the Finnish Meteorological Institute (FMI) and used by a few models.

210 Full details on the AQMEII emissions dataset are given in AQMEII documentations, available at http://aqmeii.jrc.ec.europa.eu/aqmeii2.htm. The standard emissions dataset for NA is described in the companion paper by Pierce et al. (this issue, in preparation). It is based on the 2005 U.S. National Emissions Inventory (NEI), the 2006 Canadian national inventory and the 1999 Mexican BRAVO inventory. Biogenic emissions are provided by the BEISv3.14 model, fire emissions

215 provided by daily estimates from HMS fire detection and SMARTFIRE system (year 2006) and Electric Generating Unit (EGU) point source emissions from the Continuous Emissions Monitoring data for the year 2006. The NA emissions data set did not include any dust emissions. Both the database (EU and NA) provided emissions of PM_{10} and $PM_{2.5}$, which were used by all participating groups, with the sole exception of the DEHM model, which made use of a number of different

220 emissions inventories (see Table 1).

From Section 3 onwards, the model configurations are denoted by the labels Mod1 to Mod11 for EU, and Mod12 to Mod18 for NA. In some cases the same model, but with different configurations, was run over both continents. Such is the case for the Mod3 and Mod18; Mod4 and Mod13; Mod10

225 and Mod17. No direct correspondence exists between the model labels and the model list of Table 1, for reason of anonymity.

2.3 Receptor observations for particulate matter

Particulate matter data for EU were prepared starting from hourly and daily data of total $PM_{2.5}$ and

230 PM_{10} collected by AirBase (European Air quality database, http://acm.eionet.europa.eu/databases/airbase/) and EMEP (European Monitoring and Evaluation Programme, http://www.emep.int/) networks. A total of 863 stations with valid data were made available in the ENSEMBLE database for Europe, which includes urban, sub-urban and rural stations. Too few stations measuring $PM_{2.5}$ speciation were available for year 2006 in AirBase in

235 order to be included in the Ensemble database.

Particulate matter data for NA were prepared from the data collected by the Aerometric Information Retrieval Systems (AIRS: http://www.epa.gov/air/data/aqsdb.html) and Interagency Monitoring for Protected Visual Environments, IMPROVE:

240 http://crocker.ucdavis.edu/Site/Research/AirQualityGroup/IMPROVEOverview.aspx) networks in United States, and by the National Air Pollution Surveillance (NAPS: http://www.ec.gc.ca/rnspa-naps/) network in Canada. A total of 1902 stations with valid data are available for US and Canada,

which includes urban, sub-urban and rural stations. It should be noted that not all networks provided data with the same frequency (daily of hourly), nor are the speciation data of $PM_{2.5}$ is available at all sites for all species. More details about network measurements and data quality can be found elsewhere (Appel et al., 2008; Mebust et al., 2003; Aan de Brugh 2011).

3. PM_{10} evaluation and models cross-comparison

In this section, model simulations and observations are compared for PM_{10}. To facilitate the discussions and synthesise the results, focus is given to three sub-regions of each continent. These sub-regions have been selected based on different climate and air quality characteristics, availability of measurements and previous studies (e.g., Vautard et al., this issue), and are shown in Fig 2, along with the position of PM_{10} receptor sites. For EU, sub-region 1 encompasses the north Atlantic region, the UK, Belgium, and northern of Spain. Sub-region 2, consisting of central Europe, has a continental climate with marked seasonality, many large cities, and large emissions sources. Sub-region 3, consisting of the Iberian Peninsula, was selected for the availability of measurements. For NA, sub-region 1 consists of the southwestern part of U.S. to the west of the Rocky Mountains. Sub-region 2 (Texas area), is located to the east of the Rocky Mountains. Sub-region 3, consisting of the northeastern NA including parts of Canada, has a marked seasonal cycle, three of the North American Great Lakes, the highest emissions sources in NA, and several large cities (e.g New York City, Philadelphia, Toronto, Montreal).

3.1. PM_{10} – model skill

Evolution of surface PM_{10} is shown in Fig. 2. The monthly trend is shown, based on daily data for the entire year. The time series for the each entire continent and for the three sub-regions of Figs. 1 have been analysed.

A pattern common to both continents and all sub-regions is a general underestimation of PM_{10} by the models, although there are several exceptions. For NA in particular, the underestimation is systematic across all models, though in sub-regions 2 one model slightly overestimates PM_{10} for the period of October through January. For the NA sub-region 1, model bias is severe (approximately 20 μg m^{-3}), and more marked during summer and winter. This large gap might be due to wind blown dust, which can be an important source of PM_{10} in this region (Yen et al., 2005; Park et al., 2010), but it is not accounted for in the emission inventory. In the other NA sub-regions

underestimation is milder for some models but significant for others (the worst performing model, Mod13, exhibits a bias of ~ 20 µg m^{-3} at both sub-regions 2 and 3).

280   Large biases are also observed for EU (all sub-regions), although one model (Mod1), on average, predicts PM$_{10}$ concentration of the same magnitude as observations, and Mod6 tends to overestimate the observations (except at sub-region 3). It is worth noting that the low in the observed concentrations occur during the month of August (sub-regions 1 and 2), which all models simulated with varying degrees of success. The reduced distance between PM observations and
285   simulations for the summer months, which was also found in previous studies (see eg Hodzic et al., 2005) might be explained by considering that PM winter concentrations are often driven by strong stable conditions that are not always well captured by meteorological models. It can also be noted that for sub-domain 3 the highest concentrations occur in summer, probably due to the influence of a higher rate of secondary organic aerosol formation under marked photochemical conditions and
290   possibly more wind-blown dust (Putaud et al., 2004).

Figure 3 displays the diurnal cycles for the same areas of Fig. 2. Hourly data have been used to produce these plots, averaged over the entire year. The amplitude of the diurnal cycle is generally underestimated by the majority of the models for EU and NA. One model for EU is closer to the
295   observations in terms of mean concentration and trend (Mod 6, continuous blue line in EU column of Fig. 3), except for EU sub-region 3. The models underestimate observed PM$_{10}$ during day-time hours for NA. Mod 16 (dot-dot-dash light blue line of Fig 3) is able to simulate the magnitude of PM$_{10}$ concentrations during night hours reasonable well for NA sub-regions 2 and 3.

300   The correlation, mean, error, and spread for each model simulation (entire continent) are provided in Table 2 (Table 2a for EU and Table 2b for NA) based on daily averaged data for the entire year. The correlations for the simulations vary largely (generally lower for NA than for EU), ranging from a minimum of 0.1 to a maximum 0.7 for EU Mod 7 and Mod 8. The maximum correlation for NA is 0.4 (Mod 16). For the mean PM$_{10}$ concentration the conclusions made from Figs. 2 and 3
305   hold, as the models severely underestimate PM$_{10}$, with the exception of Mod 1 and Mod 6 for EU (but they tend to overestimate PM2.5, as discussed later in Section 4.1). The variability, measured by the standard deviation of the observations, is underestimated by the NA models by a factor of two on average, indicating that the models are unable to simulate the same range in variability as the measurements. The standard deviation for the EU observed data (ST dev of 9.8 µg m^{-3}) is larger
310   than that of NA and again the models are all below the observed standard deviation (Mod 11

predicts a standard deviation six times lower). Such large differences among models depend strongly on the composition and on the components of PM_{10} included in each model's chemistry module. For example, Mod4 lacks secondary organic aerosols and wind-blown desert dust, leading to PM_{10} concentration bias among the highest.

315

We shall deepen the investigation of the model-to-model differences in the next section, with the aid of emission and deposition patterns for each model.

3.2 Models cross-comparison. Emission and deposition of PM precursors and PM pollutants

320   Analysis of emissions and deposition of several species (PM precursor and pollutants) can aid understanding of each model's internal balance and chemical transformations. The stacked distribution of quarterly accumulated emissions for five compounds is displayed in Fig. 4a (EU) and Fig. 4b (NA). Each element of the bars is the emission over a quarter of year (three months, from January to December), so that each full bar reflects the total over the year. The majority of

325   participating models (not all of them though) delivered the emission data, allowing a comprehensive analysis of PM balance. Looking at emissions for EU (Fig 4a) it emerges that, with the only exception of Mod4 which adopted a different set of emissions, and Mod6 which provided only surface emission neglecting plume rise and volumetric sources (although they were included in the runs) there are no large differences among the remaining models for SO_2, aNO_x and NH_3. Larger

330   differences, however, can be noticed for PM. Aerosol emissions differ among models, with a high variability in both the coarse (PM_{10}) and the fine ($PM_{2.5}$) components, with differences reaching ~550 and of ~200 kg km^{-2} between Mod1 and Mod7 for PM_{10} and Mod1 and Mod6 $PM_{2.5}$, respectively. Such large differences in emissions are attributable to the PM species included within each model. For example not all models include sea salt emissions. These differences, along with

335   the deposition (discussed next), are among the main responsible for the wide range of performance observed in Figs 2, 3 and Table 2. Such an influence can be observed considering, as an example, European Mod1 and Mod4. Emissions of both primary PM and precursors are among the highest as for Mod1 and among the lowest as for Mod4. This difference is clearly reflected in the computed mean concentration (see Table 2).

340

Accumulated emissions for NA also exhibit a certain degree of variability, especially for PM_{10}, with Mod13 (same emission as Mod4) showing the lower emission at all quarters. This is due to the emission inventory adopted by this model being dissimilar to the standard AQMEII emission data

sets for NA. Overall, with the further exception of low SO_2 emission by Mod18 NA emission are more homogeneous than for EU, with smoother PM differences among models.

Contributing to the final model PM concentrations is the amount of deposited substances. Playing a pivotal role are the wet and dry deposition schemes implemented in each model. Results of quarterly accumulated deposition (dry and wet, EU and NA) are shown in Figs. 5. Striking differences are mostly observed for the dry deposited substances such as $PM_{2.5}$ and the other PM secondary components in both continents. Investigating the reasons leading to the difference in deposition is not the scope of this study. Nonetheless, we note that although the dry deposition module (Table 1) is similar for all model (i.e. based on the resistance analogy schemes, Seinfeld and Pandis, 2006; Zhang et al., 2001), large deviation among models seem to indicate that the parameterisations of such scheme are rather different. This is because dry deposition is very sensitive to surface conditions (wind shear, surface roughness, temperature and radiation) and knowledge of dry-deposition processes, as well as availability of measurements, is limited (Zhang et al., 2001; 2002). Moreover, deposition schemes are coupled with chemistry and dispersion components, as well as with the treatment of the atmospheric layer just above ground level, which are treated differently by each model. Large differences in $PM_{2.5}$ deposition are mostly due to the sea-salt being included in the simulation of Mod 4,5 and 10 (EU) and Mod 12,13 and 17 (NA). Spatial maps of $PM_{2.5}$ deposition for these models (not reported) reveal that most of the deposition occurs in the ocean, whilst on land it is comparable with the other models. Mod4 and Mod 3 (which are essentially the same models as Mod13 and Mod18 for NA) exhibit PM-NO_3 deposition values higher than the other models, and Mod3 has higher values than any other participants also for PM-SO_4 (might be associated with the inclusion of sulphate from the oceans which cannot be distinguished from anthropogenic fine mode sulphate), and PM-TC (this latter together with Mod10).

Concerning the wet deposition, seasonal accumulated deposition for the soluble ions SO_4^{2-}, NO_3^-, NH_4^+ are reported in Fig. 5b (EU) and 5d (NA). Wet deposition depends mainly on the ability of models to predict the amount, duration, and type of precipitation. Vautard et al. (this issue, submitted for publication), in the context of the AQMEII activity, analysed the models performance for precipitation over NA for the year of 2006, and concluded that there is tendency to model overestimation seasonal precipitation (especially in areas of more frequent convection). This result would lead to enhance wet removal of SO_4^{2-}, NO_3^-, NH_4^+, at least for NA. Looking at the model results for wet deposition, it emerges a tendency of Mod4 and Mod5 to higher wet deposition

intensity for all species, whilst Mod17 has very low NO_3^- values. In particular Mod5 has the highest wet deposition of SO_4, NO_3 and NH_4 and the lowest dry deposition of the same specie, among all the analysed models. This might be attributed to the internal parameterisations of the model itself.

The reason for the large differences between the model results may again be attributed to the way the models internally treat the different species. Mod4, for example, calculates wet deposition of NO_3^- as the sum of the wet deposition of gaseous HNO_3 and NH_4NO_3, aerosol nitrate and organic nitrate ($H_2C(ONO_2)CHO$). Similarly, dry deposition of PM-NO_3^- is calculated as the sum of NH_4NO_3 and aerosol nitrate, based on the assumption that most of the NH_4NO_3 is in the aerosol phase. Chemistry modules within other models might have different underlying assumptions, explaining some of the spread observed in Fig 5.

3.3 Model bias

In this section we look at the PM_{10} bias and analyse possible reasons for it. We start with investigating the gas-phase precursor SO_2 and NO_2, whose calculations was also part of the AQMEII exercise. Figure 6 summarises the relationship between the mean fraction bias (MFB) and the mean fractional error (MFE) for the three sub-regions of both continents and for rural and urban receptors, with:

$$MFB = \frac{1}{N} \frac{\sum (C_m - C_{obs})}{0.5(C_m + C_{obs})} \tag{1}$$

$$MFE = \frac{1}{N} \frac{\sum |C_m - C_{obs}|}{0.5(C_m + C_{obs})} \tag{2}$$

Boylan and Russel (2006) suggested that a model performance goal (the expected level of model accuracy) for PM is met when MFE<50% and MFB< ± 30% (internal box of Fig. 6). Additionally, the model performance criteria for PM are achieved when MFE ≤ 75 % and MFB ≤ ± 60% (external box in Fig. 6). According to these targets and the results reported in Fig 4, only three models (Mod1, 6 and 10) satisfy the model goal criteria when compared against European receptors (urban and rural). Model skill target for PM_{10} NA (Fig 6, bottom row) is not reached by any model in the three sub-regions. This is due to the severe model underestimation of the NA sub-region 1, as a probable result of missing source of anthropogenic and biogenic dust. However, Mod17 has MFE and MFB within the goal target for sub-regions 2 and 3 (rural and urban receptors), and Mod 14, 15, 16 are also within the goal box for rural receptors and sub-regions 2 and 3. The alignment between bias and error emerging from Fig 6, shows that most of the uncertainty is due to bias, as already

12

410   observed in the analysis of ozone (Solazzo et al., this issue), maybe introduced by the boundary conditions or the emissions.

When looking at a similar analysis for rural receptors of SO_2 and NO_2 (Fig. 7), which are secondary regarded as secondary inorganic aerosol precursors, a similar behaviour as for PM is observed

415   (except Mod 10, all sub-regions for SO_2) in Europe, with MFB negative well aligned with MFE (lower magnitude compared to PM_{10} for the same sub-regions). For NO_2 in NA (bottom left plot of Fig 7), the trend is again similar, with the exception of sub-region 2, where NO_2 is overestimated by all models. MFE and MFB are also aligned for SO_2 (bottom right plot), although the sign of the bias varies by model and by sub-regions. The different behaviour of NO_2 and SO_2 is however not

420   surprising, as SO_2 is typically emitted by isolated point sources whose plume is not easily modelled with the current resolution of chemistry transport models. NO_2, on the other hand, derives from NO_x which is emitted at ground level by large area sources. The differences between NO_2 and SO_2 by sub-regions are thus due to the way the source distributions of the two compounds are handled in each model. We should notice that EU models that used the emission vertical distribution from

425   EMEP data base, might have a too high emission spread for point sources and other elevated sources. Large plume spread enhance depletion, thus deposition, reducing concentration. This is particularly the case for SOx, largely emitted by point sources and for the chemistry related to it (ammonium nitrate concentration is likely to increase due to reduced availability of $SO_4^=$) (e.g., Bieser et al., 2011)

430

3.3.1 PM_{10} bias and emission

We investigate here the bias induced by PM_{10} emission to modelled PM_{10} concentration. We consider four areas characterised by PM_{10} emission of increasing intensity, for EU and NA. We then analyse, for each area, the spatially averaged PM_{10} model bias at the receptors available in that area.

435   The aim is to investigate whether the PM_{10} bias decreases as the emission decreases, which would indicate that the bias is mostly due to emissions. The reference emission scenario for the entire year of 2006 has been taken from two models (Mod5 for EU and Mod16 for NA). The selection of areas of different emission intensities was based on these reference scenarios (numbered 1 to 4 in Fig. 8a for EU and 9a for NA). Receptors positioning is overlaid to the emission map of Fig. 8a and Fig. 9a.

440

The choice of the reference emission model for NA was straightforward as, among the models which provided both PM_{10} emissions and concentrations at receptors (Mod12, 16 and 17 only), emission patterns were overall quantitatively (Fig. 4b), and also geographically (in the sense of spatial distribution of sources) similar. For EU, on the contrary, Mod5 emission map was selected

as it looked the most accurate and quantitatively similar to Mod1, 3, 6 and 10 (Fig 4a). As for the selection of the areas with increasing emission intensity, the choice was driven, other then by the emissions, also by the availability of measurements. In particular, it was possible to identify three areas for each emission magnitude in NA (labelled with letters a,b,c in the figures), whilst only one area for each intensity was identified in EU. Other area of the EU continents either lacked measurements or differences among models were too high. Areas shown in Figs 8a and 9a have been selected after numerous sensitivity tests, especially for EU.

Mean fractional bias of modelled PM_{10} concentration at receptors (averaged over the pool of receptors falling in each emission area) is shown in Fig. 8b (EU) and Fig. 9b (NA). Numbers indicate the emission area, models are classified by colour. Each model bias is plotted against its own PM_{10} emission. Due to the differential emission among models presented in Fig 4a, some models show higher emission for area "2" than for area "1" (EU Mod 6 and 7) and similar intensity for area "3" and "4" (EU Mod7 and Mod8). This is, again, due to having based the analysis on a reference emission map that is not geographically the same for all models. By contrast, for the NA continent (Fig 9b), emission intensities are distributed in decreasing order (from"4" to "1"), although some overlap between areas "3" and "4". We shall point out that the concentration bias, i.e. point observation vs interpolated grid cell model concentration, might also contain some error introduced by assuming the receptor representative of an extended area. However, we are looking here at long temporal and large spatial scales for which mutual cancellation of error is expected. With this assumption in mind, we notice two different behaviours for EU and NA domains. For the former, PM_{10} concentration negative bias is smaller for regions characterised by low emission intensity (such as area "4") than for high-emission areas. MFB values for area "4" are in fact clustered between 0.2 and -0.7, whereas the average MFB for the other areas ("1" to "3") are approximately in the range 0 to -1, and show comparable, negative, values of MFB. This result might indicate that local sources have a relevant influence on PM concentration, not always well captured by regional models. It is also worth noting that differences in model performances in different areas are very clear for region 1 in EU, and that EU sub-region 1 experiences emissions higher than the other areas for all main pollutants (e.g. SO_2 and NO_X) (not shown), thus enhancing the influence of local sources on the observed concentrations.

For NA (Fig 9b), if we exclude the area "3c' of Fig 9a (characterised by high concentration bias due to wind blown dust, see Section 3.3), MFB has comparable values for all areas, between 0.1 and -1, with no reduced bias for low emission zones.

480   Some considerations might be formulated based on the results of Figs 8b and 9b. For EU, there are low- emission regions (or at least one region) for which part of the PM_{10} concentration bias can be attributed to the input emissions. The other examined areas showed a comparable MFB for all models. NA domain allows more regions to be analysed (thanks to the extension of the domain and of data availability) and the bias of PM_{10} does not depend on the PM_{10} emission data set. The

485   uniformity of MFB values for several classes of emission gives an important indication about the internal processes of the CTMs involved, and demonstrates that despite the variety of algorithms and internal parameterisations, the level of uncertainty is, overall, comparable.

It is also worth noting that differences in model performances according to the area are very clear

490   for region 1 in EU, but less for the corresponding sub-region 1 in NA. This can be explained considering that EU sub-region 1 experiences emissions higher than the other areas for all main pollutants (e.g. SO_2 and NO_X), thus enhancing the influence of local sources on the observed concentrations.

495   The above analysis tends to show that different sources of uncertainty occur in the two continents. Over EU biases are larger in high anthropogenic emission regions indicating a bias in emissions themselves or in chemistry and thermodynamics of anthropogenic compounds, while over NA the bias is rather uniform indicating a lack of background PM concentrations and therefore a possible lack of biogenic emission precursors or secondary formation from biogenic emissions. The

500   uniformity of MFB values also demonstrates that despite the variety of algorithms and internal parameterisations used, the level of skill is, overall, comparable.

3.3.2 PM_{10} and wind speed biases

505   Meteorological biases can also induce PM concentrations bias. In particular, Vautard et al. (this issue, submitted for publication) have shown that the models participating in the AQMEII exercise have a tendency to overestimate the 10 m wind speed (especially in EU), which should translate into a negative bias for concentration predictions. What is the fraction of total PM_{10} bias that can be attributed to wind speed overestimations? This issue is addressed by analysing the annual daily

510   wind speed bias against PM_{10} bias for the three regions of Figs. 1 (which are the same regions considered by Vautard et al. for studying the wind speed). It needs to be emphasised that the analysis presented is strictly valid in a spatially-averaged sense, as observed wind speed and PM_{10} concentrations are not collocated.

15

515   Results for all the participating models are reported in Fig 10a (EU) and Fig 10b (NA). Data have been averaged over the whole year and are presented for each sub-regions. In general, PM_{10} negative bias is higher when the wind speed bias is higher. Over EU this trend is marked, for each region or all regions together. Over NA, this trend is not so clear, in particular when taking each region separately, but wind biases are of smaller amplitude.

520

4. $PM_{2.5}$ and $PM_{2.5}$ components

4.1 Time series

525   Monthly time series for $PM_{2.5}$, based on 24-hour data, are shown in Fig. 11. With respect to PM_{10} (Fig 2), the model bias is much lower for both continents, demonstrating an enhanced capability of the CTMs to simulate $PM_{2.5}$.

For EU, the majority of models underestimate the monthly averaged daily $PM_{2.5}$ concentrations at 530   all sub-regions, with several exceptions. In particular, Mod1 shows an overall satisfactory agreement for all sub-regions and for the majority of the year (the high concentrations in January for sub-region 2 are not well reproduced). As was the case for PM_{10} (Fig. 2), some models estimate a pronounced peak in $PM_{2.5}$ concentrations in August which does not show up in the observed data, most probably due to fire emissions that are not taken into account by all groups.

535

Similarly to EU, the majority of NA models tend to underestimate $PM_{2.5}$, especially for sub-region 2, where only Mod17 overestimates $PM_{2.5}$ concentrations throughout the year (Fig. 11). Mod17 shows positive bias (over prediction) also at sub-region 3 and, on average, over the entire NA continent. Mods 16 and 18 underestimate $PM_{2.5}$ in the summer, but overestimate $PM_{2.5}$ throughout 540   much of the rest of the year, while all other models underestimate $PM_{2.5}$ throughout the entire year. Looking at sub-regions individually, there are models that perform satisfactorily for short periods, closely following the observations for a season, such as for example Mod18 at sub-region 1 between October and December, Mod17 for sub-region2 for April-June, and Mods 12, 15 and14 for sub-region3 for October-December. For sub-region 3 in particular, all models predict the July peak 545   and the April and October lows, although the amplitude is not well captured. Despite the enhanced model performance for $PM_{2.5}$ compared to PM_{10}, results seem to indicate that further improvements are needed to CTMs in order these to be successfully applied under a variety of conditions.

It is interesting to compare the monthly $PM_{2.5}$ and PM_{10} concentrations, as it provides indications of the proportion of the fine and coarse components of PM for each model in comparison to the observations. Results of mean $PM_{2.5}/PM_{10}$ concentration ratio, standard deviation and correlation coefficient (PCC) against the observed $PM_{2.5}/PM_{10}$ ratio for the whole continental areas are presented in Table 3. The mean ratio is overestimated by all models for both NA and EU (with the exception of Mod1 and Mod6 for EU), which is consistent with larger underestimation of PM_{10} compared to $PM_{2.5}$. Other than quantifying the bias, it is also useful to compare the association between the observed and modelled $PM_{2.5}$ to PM_{10} ratio. This ratio provides an indication of whether the models are able to reproduce the trend in the measured fine to coarse PM fraction. PCC values in Table 3 indicate that the correlation is typically below 0.5, and that in many cases the two trends are uncorrelated (exceptions being Mods 7, 8 and 11 for EU and Mods 14 and 16 for NA). As it is discussed in the next section 4.2, the correlation for $PM_{2.5}$ generally exceeds 0.4 for most models, hence the poor correlations in Table 3 are primarily due to the low or negative correlations for PM_{10}.

4.2 $PM_{2.5}$ - Model Skill

To deepen the investigation, the skill of the model to simulate the daily variability of daily mean $PM_{2.5}$ concentration is summarised in Fig. 12 (EU) and Fig. 13 (NA), for the three sub-regions (circles, square and triangles for sub-region 1,2,3 respectively). Taylor plots representation is adopted (Taylor, 2001). The ensemble mean of all available models is provided for comparison. Moreover, analysis of $PM_{2.5}$ components NH_4, SO_4, NO_3 and EC, elemental carbon) is reported in Fig. 14 for NA ($PM_{2.5}$ speciated data for EU are not widely available and therefore are not included in the analysis).

For EU, the amplitude of daily $PM_{2.5}$ variability is generally underestimated by the majority of models at all sub-regions, while the correlation with observations is always less than 0.8, with slightly better results for the rural sites. The largest underestimation in the spread occurs for EU sub-region2 (urban and rural), whereas for sub-region3 (urban and rural) the ensemble mean is among the best performing in terms of correlation coefficient (exceeding 0.6) and spread. Model correlation ranges between 0.55 and 0.75 for most models at both rural and urban stations.

Computed correlation for NA is generally higher than for EU, indicating that the daily variability of $PM_{2.5}$ is better reproduced for NA, most likely due to better PM emission datasets for NA than EU. The only exception is NA Mod18 that shows correlation values lower than 0.6 for all sub-regions.

The observed standard deviation is rather well reproduced for sub-region 2, as proved also by the ensemble mean score for this region, and to a lesser extent at sub-region 3. Conversely, a systematic worsening in model performance is observed at sub-region1.

The Taylor diagrams for inorganic aerosols and elemental carbon (Figs. 13) confirm the systematic underestimation of the standard deviation for sub-region1. By contrast, for sub-regions 2 and 3 the model performance varies depending on the PM-component being considered. Sulphate is well reproduced for both sub-regions 2 and 3, as indicated by the high correlation values (exceeding 0.7), and by the model spread which is very close to that of the observations. Nitrate is overestimated for sub-region3 and to a lesser extent for sub-region2. Conversely, ammonium is underestimated for both regions. In most cases, model performance for sulphate and nitrate are mutually compensating, meaning that underestimations in sulphate are related to overestimations in nitrate. The only exception is Mod15 overestimating both sulphate and nitrate. Finally, P-EC standard deviation is well reproduced for sub-region3, while underestimated for sub-region2. The latter analysis suggests that EC emissions are probably underestimated for NA.

Overall, poorer model skill is observed for NA sub-region1. The systematic underestimation of the computed standard deviation for all species in this region indicates there may be large emission sources missing in the emissions inventory for western NA. In addition, the western U.S. is also a challenging region to model due to its complex terrain and the close proximity of the western U.S. to western boundary of the model makes the region particularly sensitive to errors in the prescribed meteorological and chemical boundary conditions.

Finally, it is worth noting that the models showed, domain by domain, more homogenous performance for the selected compounds than for total PM$_{2.5}$ mass. This result might suggest that, while CTMs are reliable to simulate inorganic aerosol, there is still a lack in the reconstruction of some processes strongly influencing PM$_{2.5}$ concentration other than inorganic aerosol chemistry.

5. Two episodes with elevated PM concentrations

Two episodes with elevated PM concentrations in Europe and North America have been selected for a more detailed investigation of the model performance. It is of special interest to investigate if the CTMs do not only capture the average PM concentrations correctly but if they are able to reproduce peak values in the same way.

18

In Europe a period of 16 days between 13 and 28 April 2006 was chosen. During this time elevated $PM_{2.5}$ concentrations were observed at several stations in Central Europe. For the evaluation of the AQMEII model results, a region between 49° and 56° North and between 0° and 14° East was selected. Daily average $PM_{2.5}$ values were available at seven stations, four of which in Germany, and one in Denmark, Belgium and Great Britain, respectively. All stations are classified as rural stations. This type of stations typically represents the modeled concentrations, which are grid cell average values, best.

Figure 15 demonstrates that the modeled $PM_{2.5}$ concentrations scatter considerably around the observations. Except Mod4 and Mod6, all models show an increase in $PM_{2.5}$ concentrations from day 103 to day 115. The observations show a first peak on day 105 and 106 that is not well represented by the models but the high values between day 113 and day 116 are captured. The correlation coefficients are between 0.45 and 0.62 for all models except one. The bias varies between -8.8 to 12.2 $\mu g \ m^{-3}$, only 5 models show mean deviations less than 3 $\mu g \ m^{-3}$. The mean observed concentration is 15.6 $\mu g \ m^{-3}$.

In North America, the analysis could be done in a more detailed way. On one hand, at many stations hourly $PM_{2.5}$ measurements are available, but on the other hand the chemical composition is measured on a daily average basis every three to four days. This allows additional insights in the possible reasons for deviations between models and observations. The region that was chosen for the investigations was in the Eastern US between 32° and 45° North and between 72° and 92° West. Data from eighteen receptor stations, either classified as rural or suburban, was available. Six different model results could be used for the evaluation.

Between 14 July (day 195) and 29 July (day 210), high $PM_{2.5}$ values above 20 $\mu g \ m^{-3}$ were observed on several days (Fig. 16). On other days, the concentrations decreased to ~5 $\mu g \ m^{-3}$. These abrupt changes are mostly driven by transport phenomena and the models capture these changes quite well. Inaccuracies are found in the simulated timing of the episodes, e.g. the peak on day 199 is seen a bit later in the model results and another day of high PM values is modeled at the end of the period (day 209), although these high values were not observed. The correlation coefficients are between 0.42 and 0.58 for all models. These values are based on hourly concentrations and can therefore not be compared to the correlations in Europe that rely on daily averages.

The model biases are between -5.2 and +3.8 $\mu g \ m^{-3}$, corresponding to -39% to +28% with a mean observed value of 13.3 $\mu g \ m^{-3}$. This is less than in the episode that was chosen for Europe.

However, these numbers may be different for different episodes. It is interesting to note that the results from the European groups were all biased low (-5.2 to -4.3 $\mu g\ m^{-3}$) while the results for the Canadian and US groups matched the observed values better (bias between -3.4 and +3.8 $\mu g\ m^{-3}$).

The analysis of the chemical composition is based on nineteen different stations in the same area. At each station, between three and five observations were available within the 16-days period. Results from five models could be used for the comparison. This doesn't allow for a more detailed analysis than looking at the biases of the models.

The major contribution to $PM_{2.5}$ comes from sulfate, whose mean value was 6.0 $\mu g\ m^{-3}$. The European groups underestimated sulfate by 7 -17 %, while the results for the Canadian and US groups were between -11% and +21%. This points in the same direction as the results for the $PM_{2.5}$ values, although the underestimation by the European groups is lower. Nitrate showed much lower concentrations (observed value 0.5 $\mu g\ m^{-3}$) and the model results had much higher scatter around this value (-54% to + 61%). Ammonium was observed with a mean concentration of 1.8 $\mu g\ m^{-3}$. Because it is closely linked to sulfate when nitrate is low, the models showed biases in the same direction as for sulfate ranging from -36% to +30%. Again, the European groups calculated lower concentrations than the North American groups.

In summary, the chemical components sulfate, nitrate and ammonium, and in particular the sum of them, could be better reproduced by the models than total $PM_{2.5}$. Therefore, it might be that other components, like the organic aerosols, can be modeled with less accuracy than the inorganic ones. Although it is not possible to identify the main reasons for such a behaviour, it seems that the simulations performed by the North American groups were better adapted to simulate PM concentration on "their" continent, than the European counterpart.

6. Conclusions

The work presented in this paper was devoted to inter-compare and evaluate CTMs in the context of AQMEII. Focus is put on surface concentration of particulate matter (PM). Given the first-time scale of the project - involving over ten CTMs which were run over two continents (Europe and North America) for the entire 2006 year - results allow for a comprehensive analysis.

We have analysed trends of PM_{10} and $PM_{2.5}$ in several sub-regions of the continental domains, quantifying bias and model performance with the aid of statistical indicators. We conclude that a large variability among models exists (and even among different version/user of the same model),

especially for modelled PM_{10} concentration, with model estimation varying by a factor up to seven. Because most of the models shared the emissions and the atmospheric boundary conditions, reasons for the large prediction spread need to be seek elsewhere. We have analysed model's outputs in terms of emissions, dry and wet deposition of several species relevant to PM, concluding that the internal parameterisations of models play a pivotal role, although the native schemes are often similar. This is for instance the case of dry deposition, for which large difference exists, although the majority of models adopt a resistive-analogy approach. Clearly, efforts are needed to harmonise such fundamental modules of CTMs. Concerning the difference between modelled and observed PM concentrations, we observe a severe model underestimation of PM_{10} over the entire year and for all the regions, often exceeding a mean fractional error of 75%, in both continents. Additionally to the known causes of PM_{10} underestimation – unmodeled and/or unaccounted sources in the emission inventories, especially anthropogenic and natural dust – we have sought for other causes of bias. For Europe, we found that regions with low PM emission intensity have lower PM_{10} concentration bias and that a relationship exists between wind speed and PM_{10} biases. Thus, we conclude that part of bias for PM_{10} can be ascribed to PM emission and other meteorological factors, such as wind speed, at least for EU.

Evaluation of $PM_{2.5}$ concentrations shows, as expected, enhanced model performance with respect to PM_{10}, with correlation coefficients often exceeding 0.7 (higher, on average, for North America than Europe). $PM_{2.5}$ time series reveal that some models perform better than other in some areas and during some short periods of the year (seasons), but we found this behaviour not uniform is time and space. We conclude that further improvements are required in order CTMs to be successfully applied to a variety of conditions. Concerning the model skill in estimating the $PM_{2.5}$ major components (North America only) we found, domain by domain, a more homogenous performance for the selected compounds than for total $PM_{2.5}$ mass. This result might suggest that, while CTMs are reliable to simulate inorganic aerosol, there is still a lack in the reconstruction of some processes strongly influencing $PM_{2.5}$ concentration other than inorganic aerosol chemistry.

Finally, analysis of two high $PM_{2.5}$ concentration episodes in Europe and North America has revealed that, while there is a considerable scatter of model results about the observations with significant biases, models seem to be able to catch the episode peaks and the sharp oscillations around them, especially for North America. Investigation of the chemical components (North America only) shows that the chemical components sulfate, nitrate and ammonium, and in particular the sum of them, could be better reproduced by the models than total $PM_{2.5}$. Therefore, it

might be that other components, like the organic aerosols, can be modeled with less accuracy than the inorganic ones.

Acknowledgments

References

Aan de Brugh, J.M.J., Schaap, M., Vignati, E., Dentener, F., Kahnert, M., Sofiev, M., Huijnen,V., Krol, M.C., 2011. The European aerosol budget in 2006. Atmos. Chem. Phys 11, 1117-1139.

Amann, M., Bertok, I., Cofala, J., Gyarfas, F., Heyes, C., Klimon, Z., 2005. Baseline scenarios for the Clean Air for Europe (CAFÉ) Programme. Final Report, International Institute for applied systems analysis, Schlossplatz 1, A-2361 Laxenburg, Austria.

Appel, K.W., Bhave, P.V., Gilliland, A.B., Sarwar, G., Roselle, S.J., 2008. Evaluation of the Community Multiscale Air Quality (CMAQ) model version 4.5: Sensitivities impacting model performance; Part II - particulate matter, Atmospheric Environment 42, 6057-6066.

Berge, E., 1997. Transboundary air pollution in Europe. In: MSC-W Status Report 1997, Part 1 and 2, EMEP/MSC-W Report 1/97, The Norwegian Meteorological Institute, Oslo.

Bessagnet, B., Hodzic, A., Vautard, R., Beekmann, M., Cheinet, S., Honoré, C., Liousse, C., Rouil, L., 2004. Aerosol modeling with CHIMERE: preliminary evaluation at the continental scale. Atmospheric Environment 38, 2803-2817.

Bianconi, R., Galmarini, S., Bellasio, R., 2004. Web-based system for decision support in case of emergency: ensemble modelling of long-range atmospheric dispersion of radionuclides. Environmental Modelling and Software 19, 401-411.

Biesier, J., Aulinger, A., Matthias, V., Quante, M., Denier van Der Gon, H.A.C., 2011. Vertical Emission profiles for Europe based on plume rise calculations. Environmental Pollution, in press.

Binkowski, F.S. and S.J. Roselle, 2003: Models-3 Community Multiscale Air Quality (CMAQ) Model Aerosol Component 1. Model Description, J. Geophys. Res., 108(D6), 4183, doi:10.1029/2001JD001409.

Bond, T.C., E. Bhardwaj, R. Dong, R. Jogani, S. Jung, C. Roden, D.G. Streets, S. Fernandes, and N. Trautmann (2007), Historical emissions of black and organic carbon aerosol from energy-related combustion, 1850-2000, Glob. Biogeochem. Cyc., 21, GB2018

Boylan, J.W., Russell, A.G., 2006. PM and light extinction model performance metrics, goal, and criteria for three-dimensional air quality models. Atmospheric Environment 40, 4946-4959.

Brandt, J., J. H. Christensen, L. M. Frohn, C. Geels, K. M. Hansen, G. B. Hedegaard, M. Hvidberg and C. A. Skjøth, 2007. THOR – an operational and integrated model system for air pollution forecasting and management from regional to local scale. Proceedings of the 2nd ACCENT Symposium, Urbino (Italy), July 23-27, 2007

Byun, D. and K.L. Schere, 2006: Review of the Governing Equations, Computational Algorithms, and Other Components of the Models-3 Community Multiscale Air Quality (CMAQ) Modeling System. Appl. Mech. Rev., 59, 51-77.

Christensen, J. H., 1997: The Danish Eulerian Hemispheric Model – a three-dimensional air pollution model used for the Arctic, Atm. Env., 31, 4169–4191

Corbett J. J. and P. S. Fischbeck, 1997: Emissions from ships. *Science*, 278:823–824, 1997

Dennis et al., 2010. A framework for evaluating regional-scale numerical photochemical modeling systems. Environ Fluid Mech DOI 10.1007/s10652-009-9163-2

Dudhia, J. 1993 A nonhydrostatic version of the PennState/NCAR mesoscale model: Validation tests and simulation of an Atlantic cyclone and cold front. Monthly Weather Review 121, 1493-1513.

775 ENVIRON, 2010 . User's Guide to the Comprehensive Air Quality Model with Extensions (CAMx). Version 5.2.Available at: http://www.camx.com.

Erisman, J.W., Draaijers, G.P.J., Mennen, M.G., Hogenkamp, J.E.M., van Putten, E., Uiterwijk, W., Kemkers, E., Wiese, H., Duyzer, J.H., Otjes, R. and Wyers, G.P., 1996, Towards development of a deposition monitoring network for air pollution in Europe, RIVM Report 722108014, RIVM, 780 Bilthoven, The Netherlands.

Foley, K.M., S.J. Roselle, K.W. Appel, P.V. Bhave, J.E. Pleim, T.L. Otte, R. Mathur, G. Sarwar, J.O. Young, R.C. Gilliam, C.G. Nolte, J.T. Kelly, A.B. Gilliland, and J.O. Bash, 2010: Incremental testing of the Community Multiscale Air Quality (CMAQ) modeling system version 4.7. Geosci. Model Dev., 3, 205-226.

785 Forster, PM; Ramaswamy, V; et al. 2007. Changes in Atmospheric Constituents and in Radiative Forcing , In: Solomon; S; Qin, D; Manning, M; Chen, Z; Marquis, M; Averyt, KB; Tignor, M; Miller, HL (Ed) Climate Change 2007: The Physical Science Basis. Contribution of Working Group I to the Fourth Assessment Report of the Intergovernmental Panel on Climate Change, *Cambridge University Press.*

790 Gong, S.-L., Barrie, L.A., Blanchet, J.-P., 1997. Modeling sea-salt aerosols in the atmosphere. Part 1: Model development. J. Geophys. Res. 102, 3805-3818.

Gong, W., A.P. Dastoor, V.S. Bouchet, S. Gong, P.A. Makar, M.D. Moran, B. Pabla, S. Ménard, L-P. Crevier, S. Cousineau, and S. Venkatesh, 2006. Cloud processing of gases and aerosols in a regional air quality model (AURAMS). Atmos. Res. 82, 248-275.

795 Graedel, T.E., T.S. Bates, A.F. Bouwman, D. Cunnold, J. Dignon, I. Fung, D.J. Jacob, B.K. Lamb, J. A. Logan, G. Marland, P. Middleton, J.M. Pacyna, M. Placet, and C. Veldt (1993): A Compilation of Inventories of Emissions to the Atmosphere. *Global Biogeochemical Cycles.* 7, 1-26.

Guelle,, W., Schulz, M., Balkanski, Y., Dentener, F., 2001. Influence of the source formulation on meddling the atmospheeric global distribution of ´sea salt aerosol. *Journal of Geophysical Research* 106, 27509-800 27524.

Guenther, A. B., Zimmerman, P. R., Harley, P. C., Monson, R. K., Fall, R., 1993. Isoprene and monoterpene emission rate Variability: Model Evaluations and Sensitivity Analyses. *Journal of Geophysical Research* 98 (D7), 12609-12617.

Hayami, H., Sakurai, T., Han, Z., Ueda, H., Carmichael, G.R., Streets, D., Holloway, T., Wang, Z., 805 Thongboonchoo, N., Engardt, M., Bennet, C., Fung, C., Chang, A., Park, S.U., Kajino, M., Sartelet, K., Matsuda, K., Amann, M., 2008. MICS-Asia II: Model intercomparison and evaluation of particulate sulfate, nitrate and ammonium. Atmospheric Environment 42, 3510-3527.

Hodzic, A., Vautard, R., Bessagnet, B., Lattuati, M., and F. Moreto, 2005: On the quality of long-term urban particulate matter simulation with the CHIMERE model. Atmospheric Environment, 39, 5851-5864.

810 Jiang, W., 2003. Instantaneous secondary organic aerosol yields and their comparison with overall aerosol yields for aromatic and biogenic hydrocarbons. Atmospheric Environment 37, 5439–5444.

Kelly, J.T., P.V. Bhave, C.G. Nolte, U. Shankar, and K.M. Foley, 2010: Simulating emission and chemical evolution of coarse sea-salt particles in the Community Multiscale Air Quality (CMAQ) model, 815 Geosci. Model Dev., 3, 257-273.

Kim, Y., Couvidat, F., Sartelet, K., and Seigneur, C.: Comparison of different gas-phase mechanisms and aerosol modules for simulating particulate matter formation, J. Air Waste Manage. Assoc, in press, 2011.

Klimont, Z., et al. 2009. Projections of SO2, NOx and carbonaceous aerosols emissions in Asia. Tellus, 61B, 820 602-617.

Lamarque, J.F., Bond, T.C., Eyring, V., Granier, C., Heil, A., Klimont, Z., Lee, D., Liousse, C., Mieville, A., Owen, B., Schultz, M.G., Shindell, D., Smith, S.J., Stehfest, E., Van Aardenne, J., Cooper, O.R., Kainuma, M., Mahowald, N., McConnell, J.R., Naik, V., Riahi, K., Van Vuuren, D.P., 2010. Historical (1850-2000) gridded anthropogenic and biomass burning emissions of reactive gases and aerosols: 825 Methodology and application. Atmospheric Chemistry and Physics Discussions 10, 4963-5019.

Loosmore, G., Cederwall, R., 2004. Precipitation scavenging of atmospheric aerosols for emergency response applications: testing an updated model with new real-time data. Atmospheric Environment 38, 993–1003.

Makar, P.A., Bouchet, V.S., Nenes, A., 2003: Inorganic chemistry calculations using HETV – a vectorized solver for the SO_4^{2-}–NO_3^-–NH_4^+ system based on the ISORROPIA algorithms. *Atmos. Environ.* 37, 2279-2294.

Mallet V., Quélo D., Sportisse B., Ahmed de Biasi M., Debry E., Korsakissok I., Wu L., Roustan Y., Sartelet K., Tombette M., and Foudhil H., 2007. Technical Note: The air quality modeling system Polyphemus. Atmos. Chem. Phys., 7, 5479-5487.

Manders, A.M.M., Schaap, M., Hoogerbrugge, R., 2009. Testing the capability of the chemistry transport model LOTUS-EUROS to forecast PM10 levels in the Netherlands. Atmospheric Environment 43, 4050-4059.

Mårtensson E.M., Nilsson E.D., de Leeuw G., Cohen L.H and Hansson H-C, Laboratory simulations and parameterisation of the primary marine aerosol production, J. Geophys. Res., 108(D9), 4297, doi:10.1029/2002JD002263, 2003.

Mebust, M.R., Eder, B.K., Binkowski, F.S., Roselle, S.J., 2003. Models-3 Community Multiscale Air Quality (CMAQ) model aerosol component. 2. Model evaluation. Journal of Geophysical Research 108, D6, 4184, doi:10.1029/2001JD001410.

Monahan, E.C., Spiel, D.E., Davidson, K.L., 1986. In: Monahan, E.C., Mac Niocaill, G. (Eds.), Oceanic Whitecaps. Riedel, Norwell, MA, pp. 167–174.

Nenes, A., Pilinis, C., and Pandis, S.: ISORROPIA: A new thermodynamic equilibrium model for multicomponent inorganic aerosols, Aquat. Geochem., 4, 123-152, 1998.

Park, S. H., Gong, S. L., Gong, W., Makar, P. A., Moran, M. D., Zhang, J., Stroud, C. A., 2010. Relative impact of windblown dust versus anthropogenic fugitive dust in $PM_{2.5}$ on air quality in North America, *J. Geophys. Res.*, 115, D16210, doi:10.1029/2009JD013144.

Philipona R, Behrens K, Ruckstuhl C (2009) How declining aerosols and rising greenhouse gases forced rapid warming in Europe since the 1980s. Geophys. Res. Lett. 36:doi:10.1029/2008GL036350

Pierce, T., Pouliot, G., Denier van der Gone, D., Schaap, M., Moran, M., and et al. Comparing Emission Inventories and Model-Ready Emission Datasets between Europe and North America for the AQMEII Project. Submitted for publication

Pun, B., C. Seigneur and K. Lohman (2006) Modeling secondary organic aerosol via multiphase partitioning with molecular data, Environ. Sci. Technol., 40, 4722-4731.

Putaud, J.-P., Raes, F., Van Dingenen, Bruggemann, E., and et al., 2004. A European aerosol phenomenology – 2 : Chemical characteristics of particulate matter at kerbside, urban, rural and background sites in Europe. Atmospheric Environment 38, 2579-2595.

Rao, S.T., Galmarini, S., Puckett, K., 2011. Air quality model evaluation international initiative (AQMEII). Bulletin of the American Meteorological Society 92, 23-30. DOI:10.1175/2010BAMS3069.1

Renner, E., Wolke, R., 2010. Modelling the formation and atmospheric transport of secondary inorganic aerosols with special attention to regions with high ammonia emissions. Atmos. Environ. 41, 1904–1912.

Renner, E., Wolke, R., 2010. Modelling the formation and atmospheric transport of secondary inorganic aerosols with special attention to regions with high ammonia emissions. *Atmospheric Environment* 44(15), 1904–1912.

Sartelet K., Debry E., Fahey K., Roustan Y., Tombette M., Sportisse B., 2007. Simulation of aerosols and gas-phase species over Europe with the Polyphemus system. Part I: model-to-data comparison for 2001. Atmospheric Environment, 41 (29), 6116-6131, doi:10.1016/j.atmosenv.2007.04.024.

Sartelet, K., Debry, E., Fahey, K., Roustan, Y., Tombette, M. and Sportisse, B.: Simulation of aerosols and gas-phase species over Europe with the Polyphemus system. Part I: model-to-data comparison for 2001, Atmospheric Environment, 41 (29), 6116-6131, doi:10.1016/j.atmosenv.2007.04.024, 2007.

Schaap, M., Timmermans, R.M.A., Roemer, M., Boersen, G.A.C., Builtjes, P.J.H. Sauter, F.J., Velders, G.J.M. and Beck, J.P. (2008) The LOTOS–EUROS model: description, validation and latest developments', Int. J. Environment and Pollution, Vol. 32, No. 2, pp.270–290.

Schaap, M., Timmermans, R.M.A., Sauter, F.J., Roemer, M., Velders, G.J.M., and et al. 2008. The LOTOS-EUROS model: description, validation and latest developments. Int. J. environ. Pollut. 32, 270-290.

Schell B., I.J. Ackermann, H. Hass, F.S. Binkowski, and A. Ebel (2001), Modeling the formation of secondary organic aerosol within a comprehensive air quality model system, *Journal of Geophysical research* 106, 28275-28293.

Schultz, M. G., A. Heil, J. J. Hoelzemann, A. Spessa, K. Thonicke, J. Goldammer, A. C. Held, and J. M. Pereira, 2008. Global emissions from wildland fires from 1960 to 2000. *Global Biogeochemical Cycles*, 22:B2002, April 2008.

Seinfeld, J., and S. Pandis, Atmospheric Chemistry and Physics, 1326 pp., Wiley, New York, 2006.

Simpson, D., Fagerli, H., Jonson, J.E., Tsyro, S., Wind, P., and Tuovinen, J.-P., 2003. The EMEP Unified Eulerian Model. Model Description. Technical Report EMEP MSC-W Report 1/2003,.The Norwegian Meteorological Institute, Oslo, Norway.

Simpson, D., Fagerli, H., Jonson, J. E., Tsyro, S., Wind, P., and Tuovinen J-P 1-8-2003, Transboundary Acidification, Eutrophication and Ground Level Ozone in Europe, PART I, Unified EMEP Model Description. pp. 104.

Skamarock, W.C., Klemp, J.B., Dudhia, J., Gill, D.O., Barker, D.M., Wang, W., Powers, J.G., 2008. A description of the Advanced Research WRF Version 2. NCAR technical note NCAR/TND468+STR.

Smith, S. J., Pitcher, H., and Wigley, T.M.L. (2001) Global and Regional Anthropogenic Sulfur Dioxide Emissions. Global and Planetary Change, 29, pp 99-119

Smyth, S.C., W. Jiang, H. Roth, M.D. Moran, P.A. Makar, F. Yang, V.S. Bouchet, and H. Landry, 2009: A comparative performance evaluation of the AURAMS and CMAQ air quality modelling systems. Atmos. Environ., 43, 1059-1070.

Sofiev, M., A model for the evaluation of long-term airborne pollution transport at regional and continental scales, Atmos. Env., 34(15), pp. 2481-2493, 2000.

Sofiev, M., Siljamo, P., Valkama, I., Ilvonen, M., Kukkonen, J., 2006. A dispersion modeling system SILAM and its evaluation against ETEX data. Atmospheric Environment 40, 674-685

Sofiev, M., Soares, J., Prank, M., de Leeuw, G., Kukkonen, J., A regional-to-global model of emission and transport of sea salt particles in the atmosphere, submitted for publication in Journal of Geophysical Research - Atmospheres, 2011

Stern, R., Builtjes, P., Schaap, M., Timmermans, R., Vautard, R., Hodzic,A., Memmesheimer, M., Feldmann, H., Renner, E., Wolke, R., Kerschbaumer,A., 2008. A model inter-comparison study focussing on episodes with elevated PM10 concentrations. Atmospheric Environment 42, 4567-4588

Stohl, A., Williams, E., Wotawa, G., Kromp-Kolb, H., 1996. A European inventory of soil nitric oxide emissions and the effect of these emissions on the photochemical formation of ozone, Atmospheric Environment 30, 3741-3755.

Strand, A., Hov, O., 1996. The impact of man-made and natural NOx emissions on upper tropospheric ozone: A two-dimensional model study. Atmospheric Environment 8, 1291-1303.

Taylor, K.E., 2001. Summarising multiple aspects of model performance in a single diagram. J. Geophys. Res. 106, 7183-7192.

van Loon, M., Vautard, R., Schaap, M., Bergström, R., Bessagnet, B., Brandt, J., and et al. 2007. Evaluation of long-term ozone simulations from seven regional air quality models and their ensemble average. Atmos. Environ. 41, 2083-2097.

Vautard, R., M. Schaap, R Bergström, B. Bessagnet, J. Brandt, P.J.H. Builtjes, J.H. Christensen, C. Cuvelier, V. Foltescu, A. Graf, A. Kerschbaumer, M. Krol, P. Roberts, L. Rouïl, R. Stern, L. Tarrason, P. Thunis, E. Vignati, P. Wind, 2009, Skill and uncertainty of a regional air quality model ensemble. Atmos. Environ., 43, 4822-4832.

Vautard, R., Moran, M.D., Solazzo, E., Gilliam, R.C., Matthias, V., et al. Evaluation of the meteorological forcing used for AQMEII air quality simulations. *Submitted for publication to Atmospheric Environment (this issue)*

Vautard, R., Yiou, P., and G. J. van Oldenborgh, 2009: Decline of fog, mist and haze in Europe over the past 30 years, Nature Geoscience, 2, 115-119.

Vestreng V, Støren E. Analysis of the UNECE/EMEP Emission Data. MSC-W Status Report 2000. Norwegian Meteorological Institute: Blindern, Oslo; 2000.

Wolke, R., Knoth, O., Hellmuth, O., Schröder, W., Renner, E. 2004. The parallel model system LM-MUSCAT for chemistry-transport simulations: Coupling scheme, parallelization and applications. Parallel Computing, 363–370

Wolke, R., Knoth, O., Hellmuth, O., Schröder, W., Renner, E. 2004. The Parallel Model System LM-MUSCAT for Chemistry-Transport Simulations: Coupling Scheme, Parallelization and Applications. In *Parallel Computing*, b363–370. Elsevier, 2004.

Yin, D., Nickovic, S., Barbaris, B., Candy, B., Sprigg, W.A., 2005. Modeling wind-blown desert dust in the southwestern United States for public health warning: A case study. Atmospheric Environment 39, 6243–6254.

Yiou, P., G.-J. Van Oldenborgh and R. Vautard, 2011: Trends of fog, mist and haze over the past 30 years and regional warming, Atmospheric Environment, submitted.

Zhang, L., Gong, S., Padro, J., Barrie, L., 2001. A size-segregated particle dry deposition scheme for an atmospheric aerosol module. Atmospheric Environment 549–560.

Zhang, L., Moran, M.D., Makar, P.A., Brook, J.R., Gong, S., 2002. Modelling gaseous dry deposition in AURAMS: a unified regional air-quality modeling system. Atmospheric Environment 36, 537-560

Captions

Figures

Figure 1a. Three sub-regions for EU (daily and hourly receptors shown).

Figure 1b. Three sub-regions for NA (daily and hourly receptors shown).

Figure 2 PM_{10} 24-hour monthly time series for the whole continent (top row), sub-regions 1 to 3 (second to fourth row). Left column EU and right column NA (observation is the line with symbols)

Figure 3 PM_{10} daily cycle for the whole continent (top row), sub-regions 1 to 3 (second to fourth row). Left column EU and right column NA (observation is the line with symbols)

Figure 4a – Quarterly accumulated emissions for EU continental domain

Figure 4b – Quarterly accumulated emissions for NA continental domain

Figure 5a - Quarterly accumulated dry deposition for EU continental domain

Figure 5b - Quarterly accumulated wet deposition for EU continental domain

Figure 5c - Quarterly accumulated dry deposition for NA continental domain

Figure 5d - Quarterly accumulated wet deposition for NA continental domain

Figure 6- MFB vs MFE for PM_{10} in Europe (top row) and North America (bottom row), at urban (left column) and rural (right column) sites.

Figure 7 - MFB vs MFE for NO_2 (left column) and SO_2 (right column) in Europe (top row) and North America (bottom row).

Figure 8a – Annual averaged PM_{10} emission over Europe and areas used for analysis (see text for details). PM_{10} receptors are also shown (grey symbols)

Figure 8b – Analysis of bias in the emission areas of Fig 8a as function of PM_{10} emission (see text for detail).

Figure 9a. Annual averaged PM_{10} emission over North America and areas used for analysis (see text for details). PM_{10} receptors are also shown (white dots)

Figure 9b. Analysis of bias in the emission areas of Fig 9a as function of PM_{10} emission (see text for detail).

Figure 10. PM10 concentration MFB vs wind speed MFB, averaged over all year and over the three sub-regions for Fig 1 for *a)* EU and *b)* NA (Square: Dom1; Triangle: Dom2; Circle: Dom3)..

Figure 11. $PM_{2.5}$ 24-hour monthly time series for the whole continent (top row), sub-regions 1 to 3 (second to fourth row). Left column EU and right column NA (legend on the right)

Table 1

Model	Aerosol size	Inorganic module	Organic module	Sea salt module	Wet dep.	Dry dep.	Emi	BC	Vertical resolution	Other
MM5 Chimere	40 nm to 10 μm (8 bins)	ISORROPIA[2]	Pun et al 2006.; SOA isoprene chemistry	Monahan et al 1986	In cloud and sub cloud scavenging for gases and particles	Gas: Emberson et al. for gas;: resistive approach for particles	standard	standard	9 levels (first: 20 m)	
MM5 Polyphemus	0.01μm to 10μm (5 bins)	ISORROPIA[1]	SuperSorgam (Kim et al. 2011)	Monahan et al 1986	Washout coefficient (with parameters from Loosmore and Cederwall; Sartelet et al 2001.)	Zhang et al. (2001)	standard[3]	standard	9 levels from surface to 1200	
WRF(NA) MM5 (EU) CAMx	$PM_{2.5}$ $PM_{2.5-10}$	ISORROPIA[1]	SOAP semi-volatile scheme with aging	Emission input (Environ)	CAMx rainout and washout	Zhang scheme for gases and particles	standard	standard	26 (23) first: 40 (30) m NA (EU)	CB05 Chemical Mechanism
COSMO Muscat	$PM_{2.5}$ $PM_{2.5-10}$	Renner and Wolke (2010)	SORGAM (Schell et al., 2001)	Guelle et al. (2003)	Berge (1997)	Resistive Seinfeld and Pandis	standard[4]	standard	22 layers (first: 60 m)	Wolke et al. (2004)
ECMWF SILAM	$PM_{2.5}$ and PM_{10}; sea salt – 5 bins from 0.01 to 30 mkm	Updated DMAT model (Sofiev, 2000), includes SO_4, NO_3, NH_4	None	SILAM native scheme (Sofiev et al, 2011)	Scavenging coefficient parameterization	Resistive (Seinfeld and Pandis, 1998)	standard	Standard; own boundaries for sea salt	9 layers with varying thickness; top: 10 km	

Model	Size distribution	Thermodynamics	SOA/VOC	Sea-salt	Scavenging	Dry deposition	Emissions	Boundary conditions	Vertical layers	Notes
MM5 DEHM	2 size bins (1-2.5, 6-10 µm diameter). No particle dynamics.	Modified version of Strand and Hov (1994),	similar to the EMEP model (Simpson et al., 2003).	1 size bin mean 6 µm diameter	In cloud, below cloud scavenging coefficients (Christensen, 1997)	Resistive method	Several sources[5]	Nested in a hemispheric model	29 layers, top: 100 hPa	Two-way nesting between hemispheric and NA/EU domains (Frohn et al., 2002)
WRF CMAQ	Trimodal size distribution (Binkowski and Roselle 2003)	ISORROPIA[1]	Foley et al	Kelly et al. (2010)	Derived from that of RADM (see Byun and Schere, 2006)	Resistance law concept (see Byun and Schere, 2006)	standard	standard	34 layers, first: 25 m	
ECMWF LOTOS-EUROS	1 size bin (0-2.5um); also 2.5-10um for sea-salt	ISORROPIA[1]	None	Monahan 1986, Martensson 2003	Simpson, 2003	Resistance approach; aerosol resistances following EDAC (Erisman 1994)	Standard	Standard	4 layers (surface, boundary layer, 2 residual layers)	Forest fire emissions using data from FMI/Silam (Sofiev 2011) Model description in (Schaap 2008)
GEM AURAMS	0.01 µm to 41 µm (diameter; 12 bins)	HETV (Makar et al., 2003) based on ISORROPIA[1]	Jiang (2003); 7 lumped VOC precursor species	Gong et al. (1997)	In-cloud and below-cloud scavenging for gases and particles (Gong et al., 2006)	Zhang et al. (2001)	quasi-standard (same inventories, own processing); BEIS v3.09	Climatological profiles	29 levels (first layer: 15 m)	Explicit treatment of nucleation, condensation, coagulation, swelling, activation; ADOM-2 gas-phase mechanism
COSMO-CLM CMAQ	Trimodal size distribution (Binkowski and Roselle)	ISORROPIA[1]	SORGAM (Schell et al., 2001)	Wind speed driven (Monahan et al.)	see Byun and Schere, 2006	Resistance approach	standard	standard	30 layers, first 36 m	CBIV gas pahse chemistry for Europe, CB05 chemistry for NA

[5] Global: IPCC RPC 3-PD Lamarque et al (2010), Bond et al (2007), Smith et al (2001); Ships: Corbett and Fischbeck (1997); GEIA natural emissions (Graedel et al. 1993), Wildfires: Schultz et al. Europe: EMEP (Vestreng and Støren, 2000)

Table 2a

		RMSE	PCC	Mean	St Dev
PM$_{10}$ daily averaged hourly data	**Mod1**	10.4	0.3	23.7	5.5
	Mod2	20.5	0.5	9.2	2.7
	Mod3	15.3	0.3	13.4	3.8
	Mod4	21.7	0.6	7.9	2.2
	Mod5	15.3	0.4	15.6	7.5
	Mod6	11.5	0.1	29.3	7.4
	Mod7	15.3	0.7	14.4	4.7
	Mod8	21.4	0.7	7.9	3.0
	Mod9	18.7	0.4	11.4	4.0
	Mod10	12.7	0.4	18.8	5.6
	Mod11	19.0	0.1	9.0	1.7
	Observation			27.7	9.8

Table 2b

		RMSE	PCC	Mean	St Dev
PM$_{10}$ daily averaged hourly data	**Mod12**	20.9	0.3	10.5	2.0
	Mod13	25.6	0.3	5.7	1.6
	Mod14	17.2	0.2	14.5	3.0
	Mod15	17.5	0.2	14.2	3.2
	Mod16	19.9	0.4	11.5	2.2
	Mod17	5.3	0.15	20.1	2.9
	Observation			30.7	5.4

Table 3a

EU (n = 12)	Mean	Std Dev	PCC
Obs	0.67	0.09	
Mod3	0.81	0.10	0.11
Mod4	0.89	0.03	< 0.1
Mod5	0.89	0.07	< 0.1
Mod6	0.61	0.05	< 0.1
Mod7	0.73	0.06	0.70
Mod8	0.85	0.05	0.60
Mod9	0.82	0.06	0.35
Mod10	0.90	0.05	< 0.1
Mod1	0.63	0.10	0.13
Mod2	0.92	0.03	0.30
Mod11	0.90	0.02	0.52

Table 3b

NA (n =12)	Mean	Std Dev.	PCC
Obs	0.49	0.03	
Mod12	0.94	0.05	< 0.1
Mod13	0.91	0.15	0.17
Mod14	0.81	0.03	0.39
Mod16	0.96	0.16	0.39
Mod17	0.91	0.04	0.01
Mod15	0.84	0.04	0.16

Figures
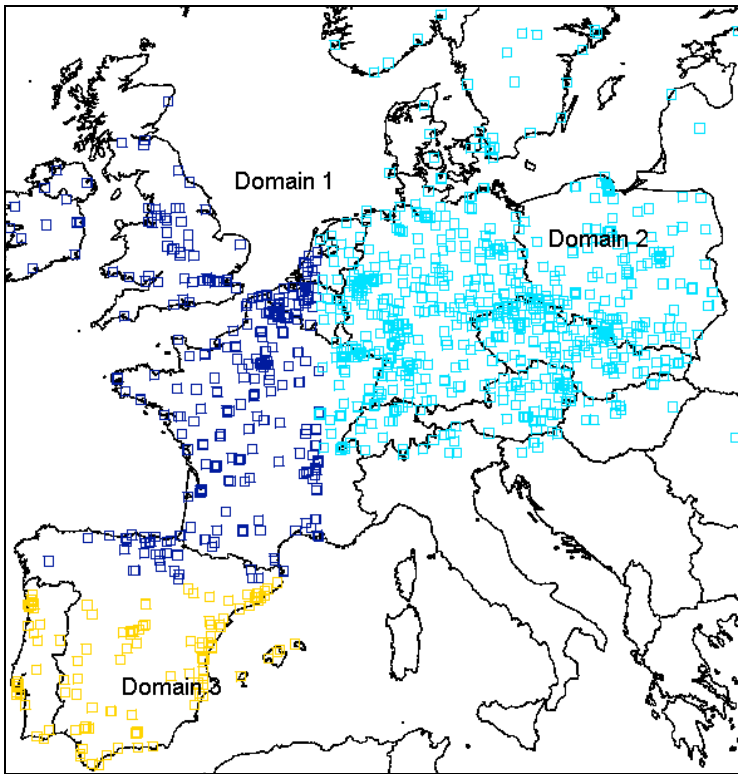
Figure 1a.
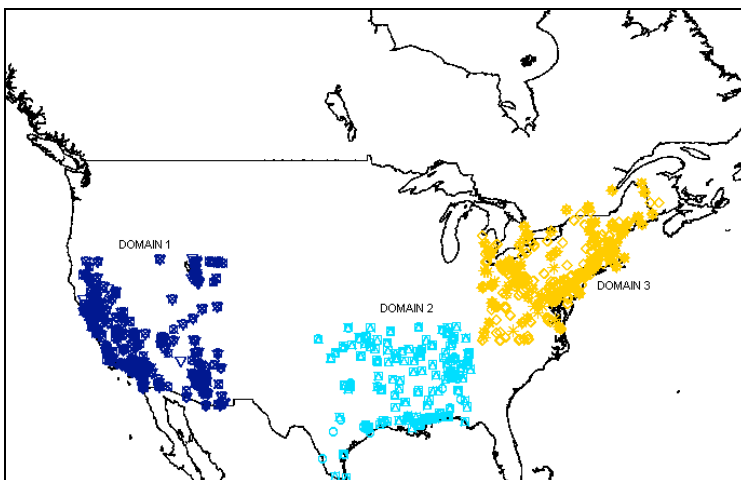
Figure 1b.
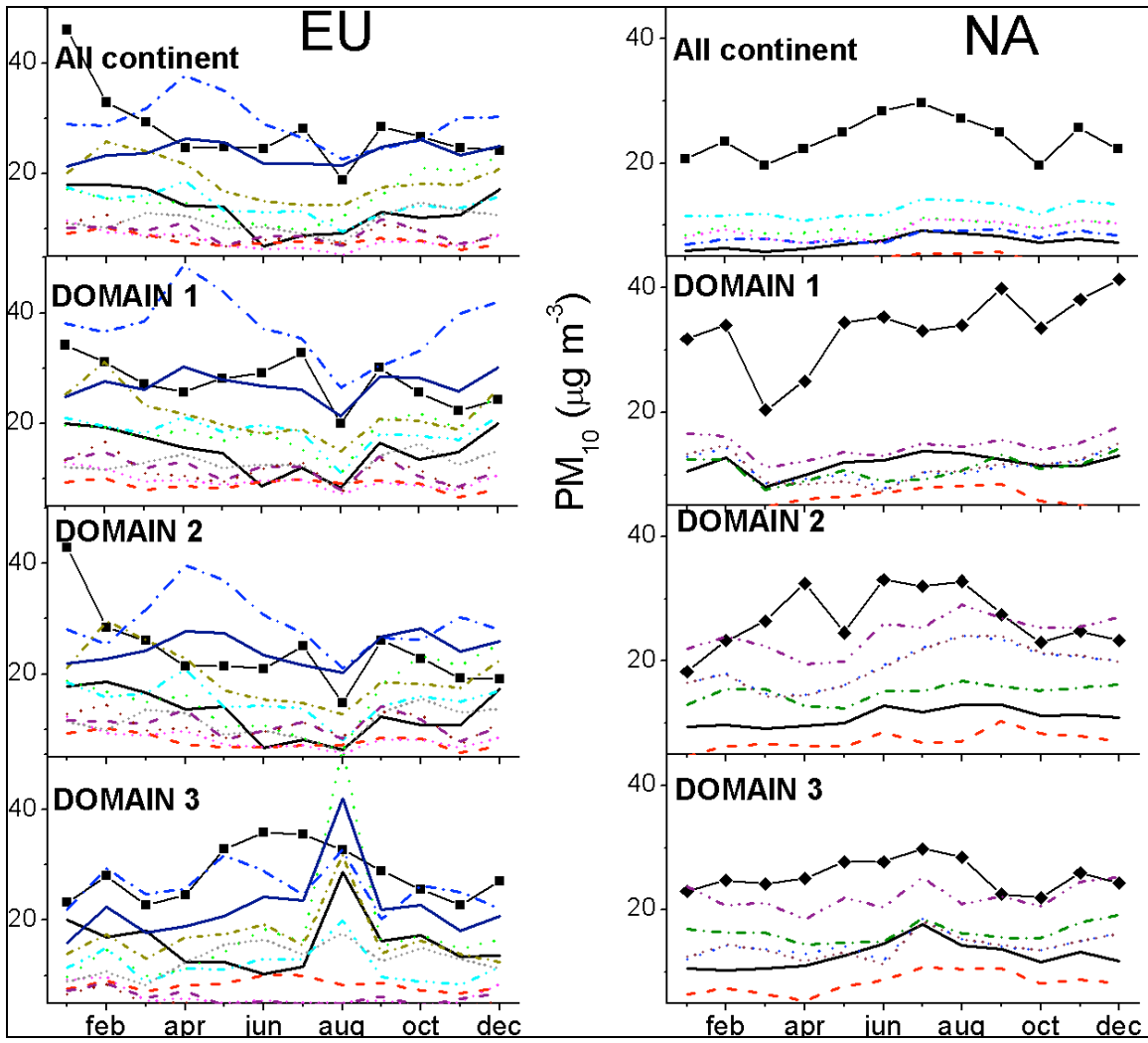
Figure 2
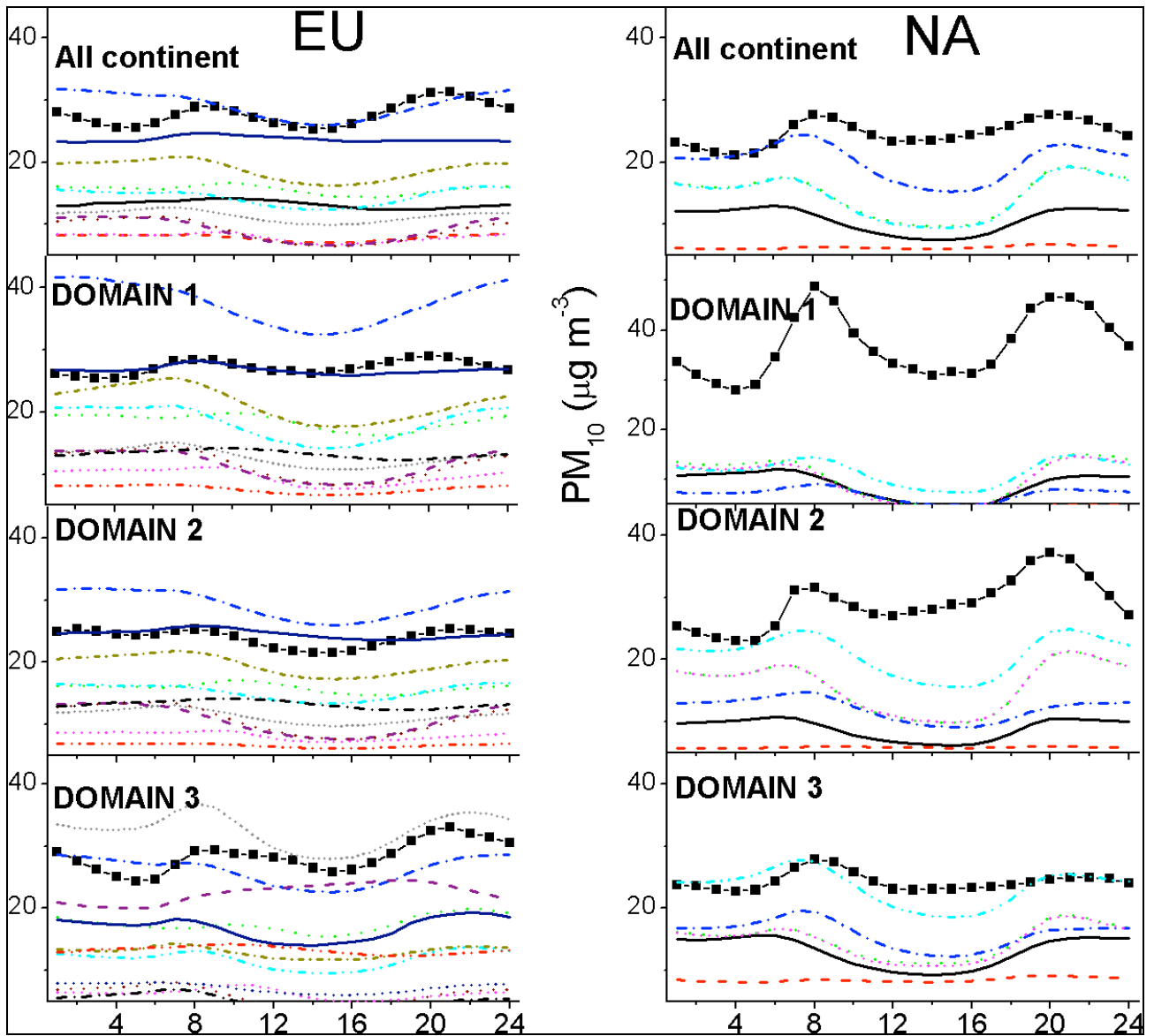
Figure 3
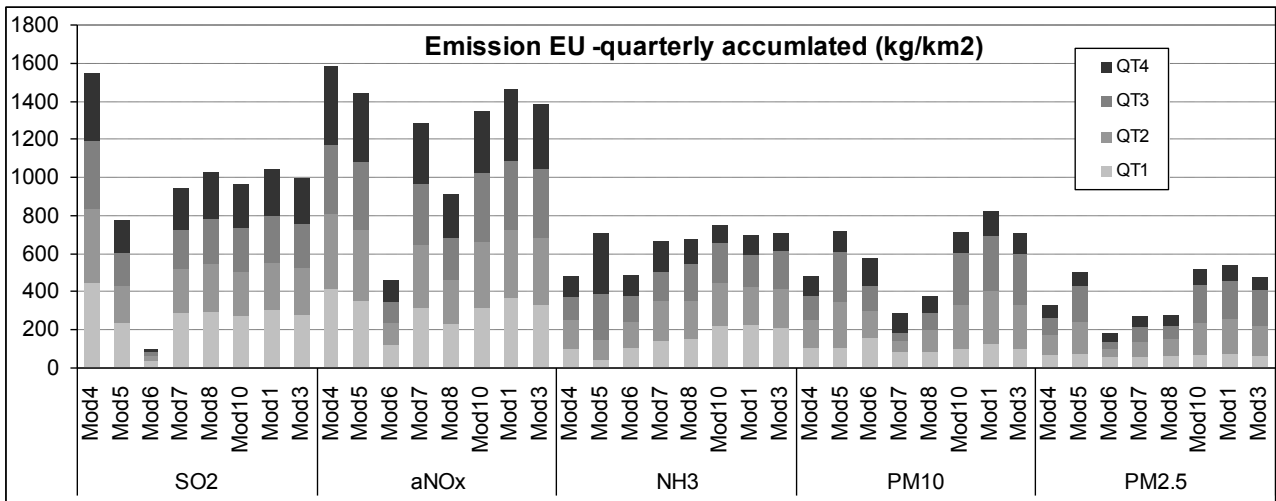
Figure 4a –
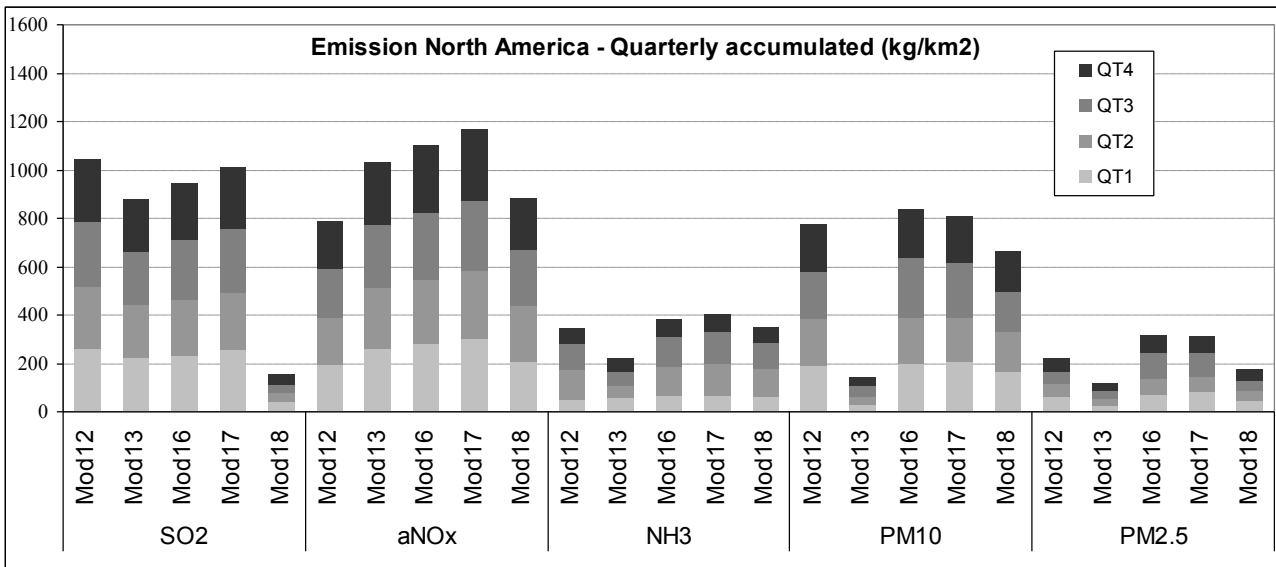
Figure 4b –
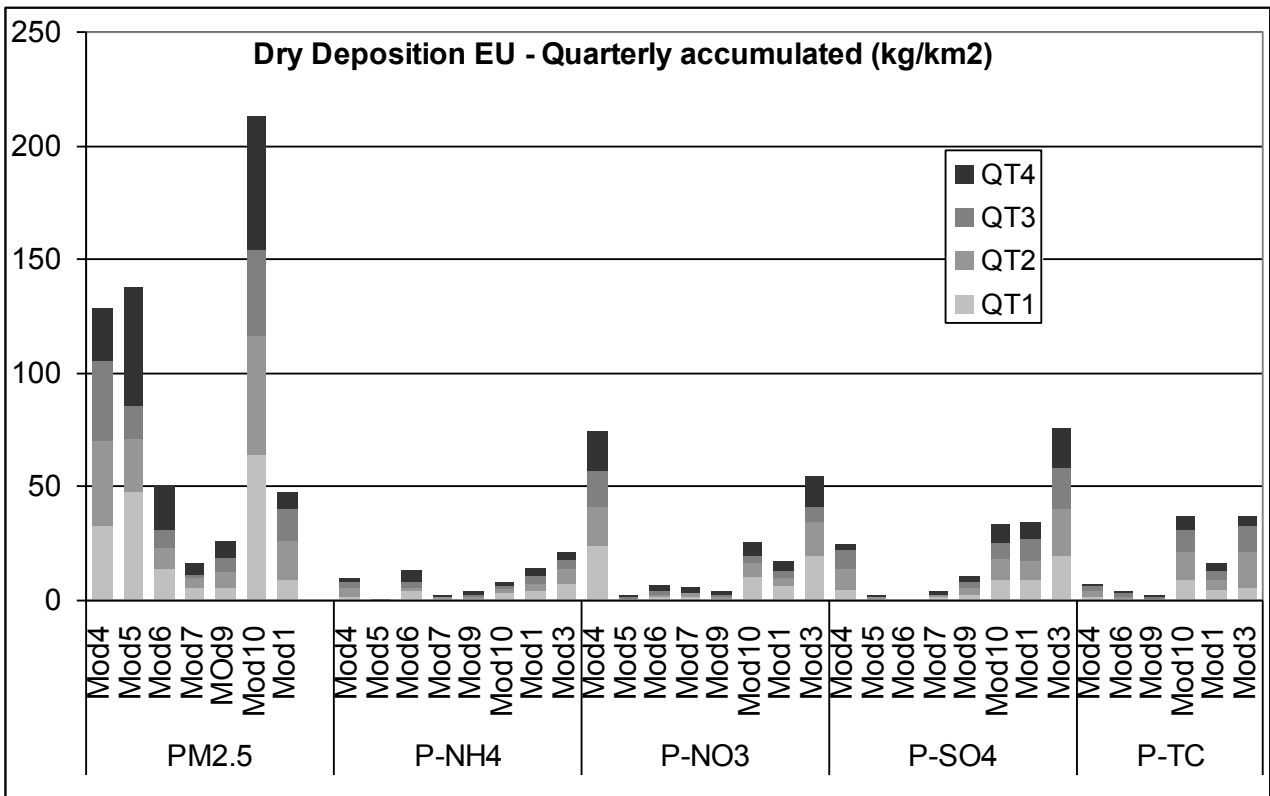
Figure 5a
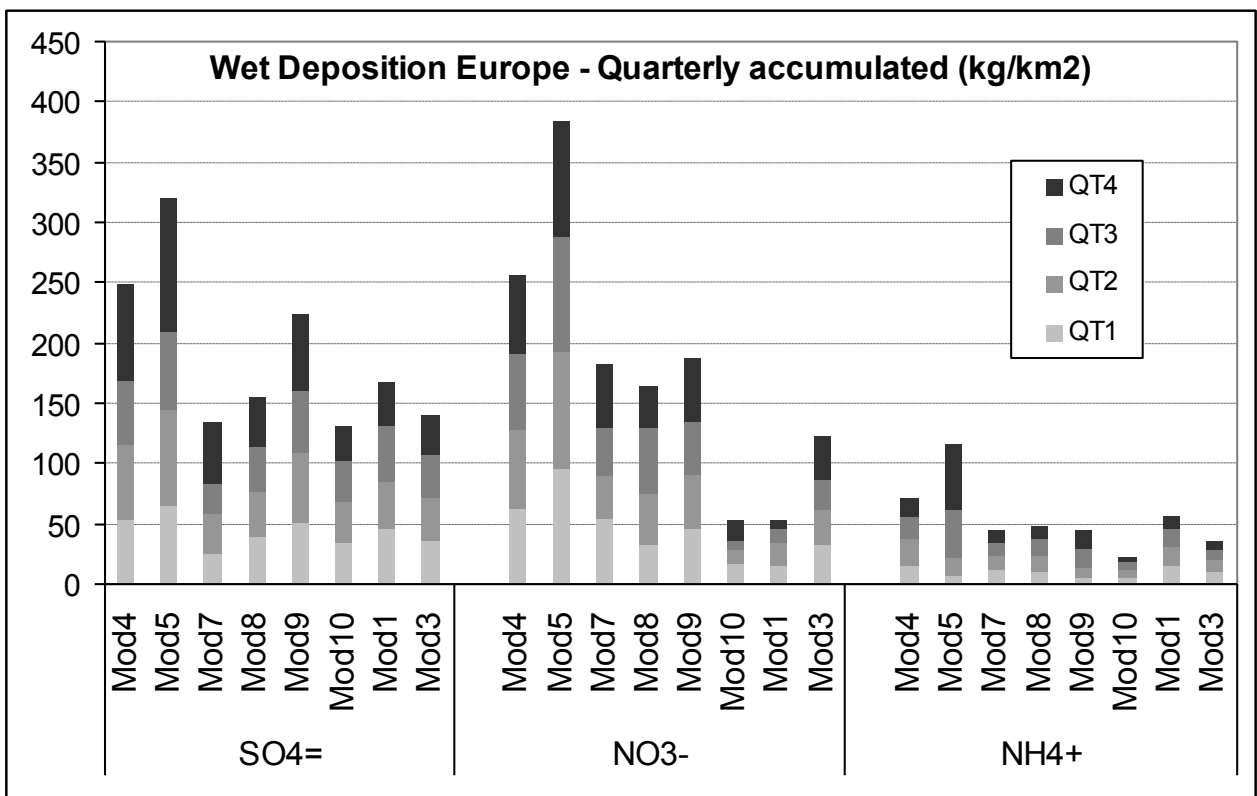
Figure 5b
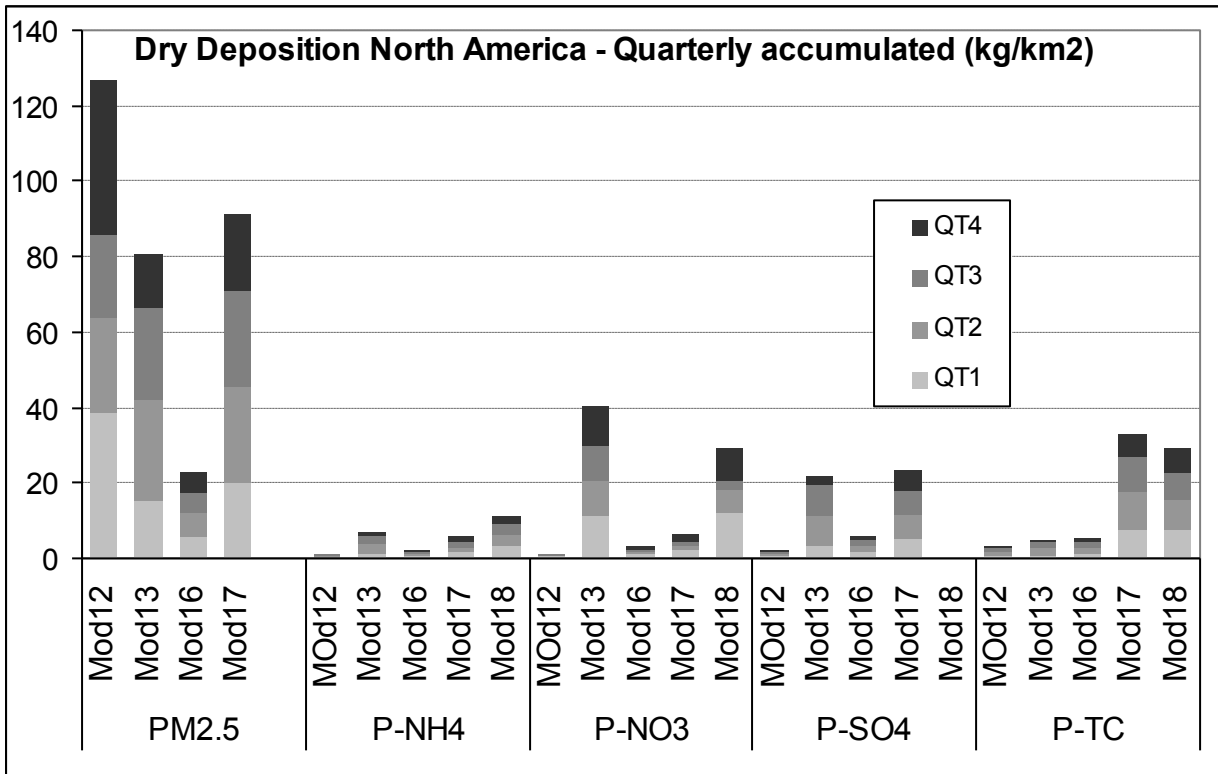
Figure 5c
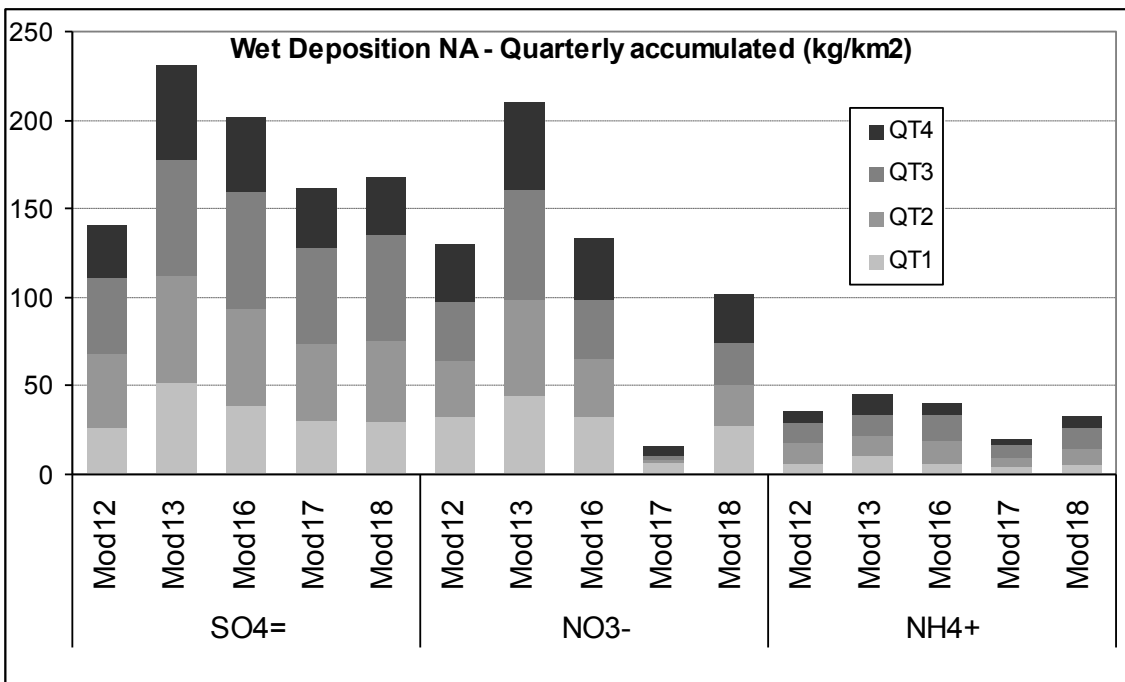
Figure 5d
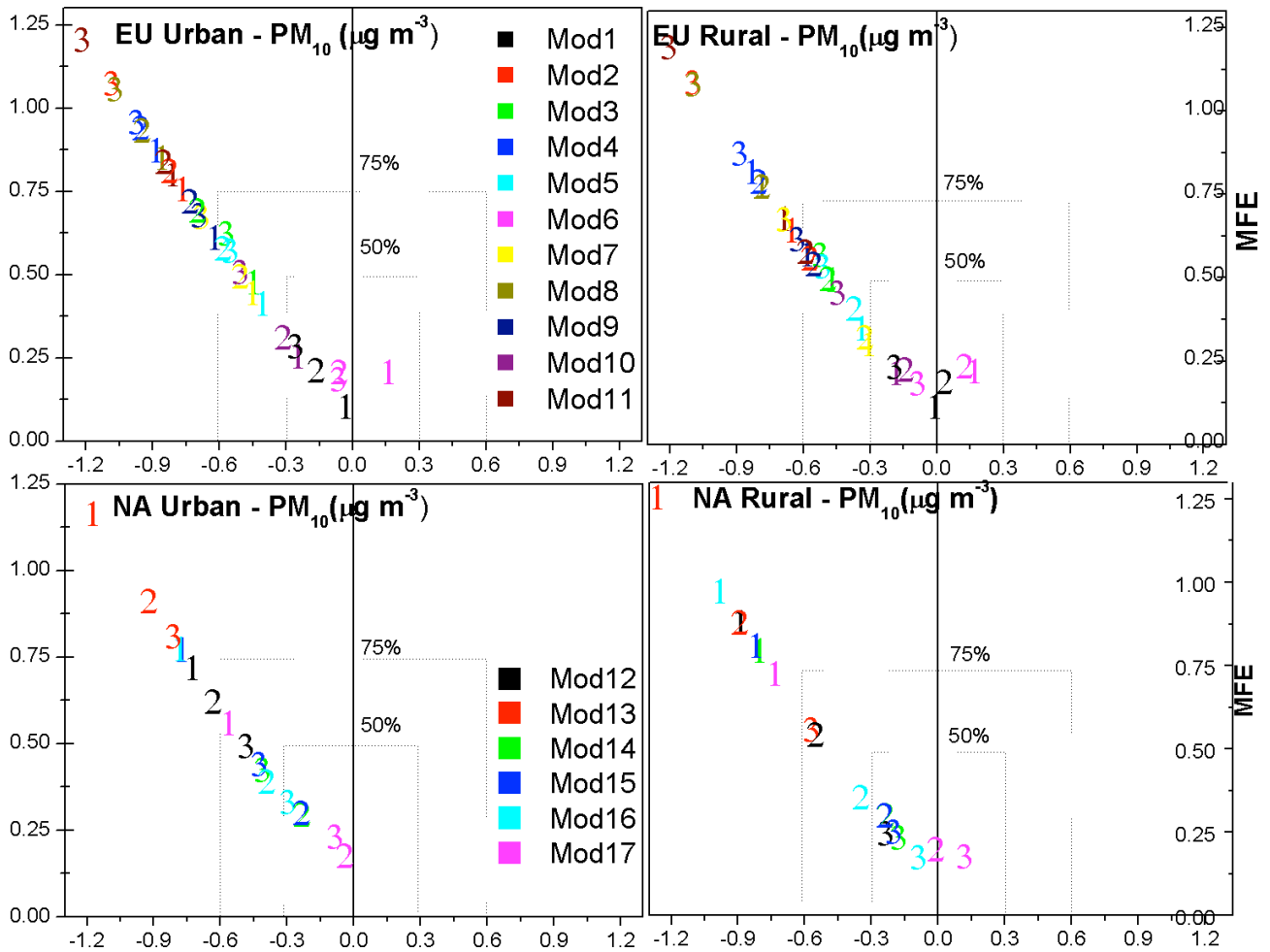
Figure 6
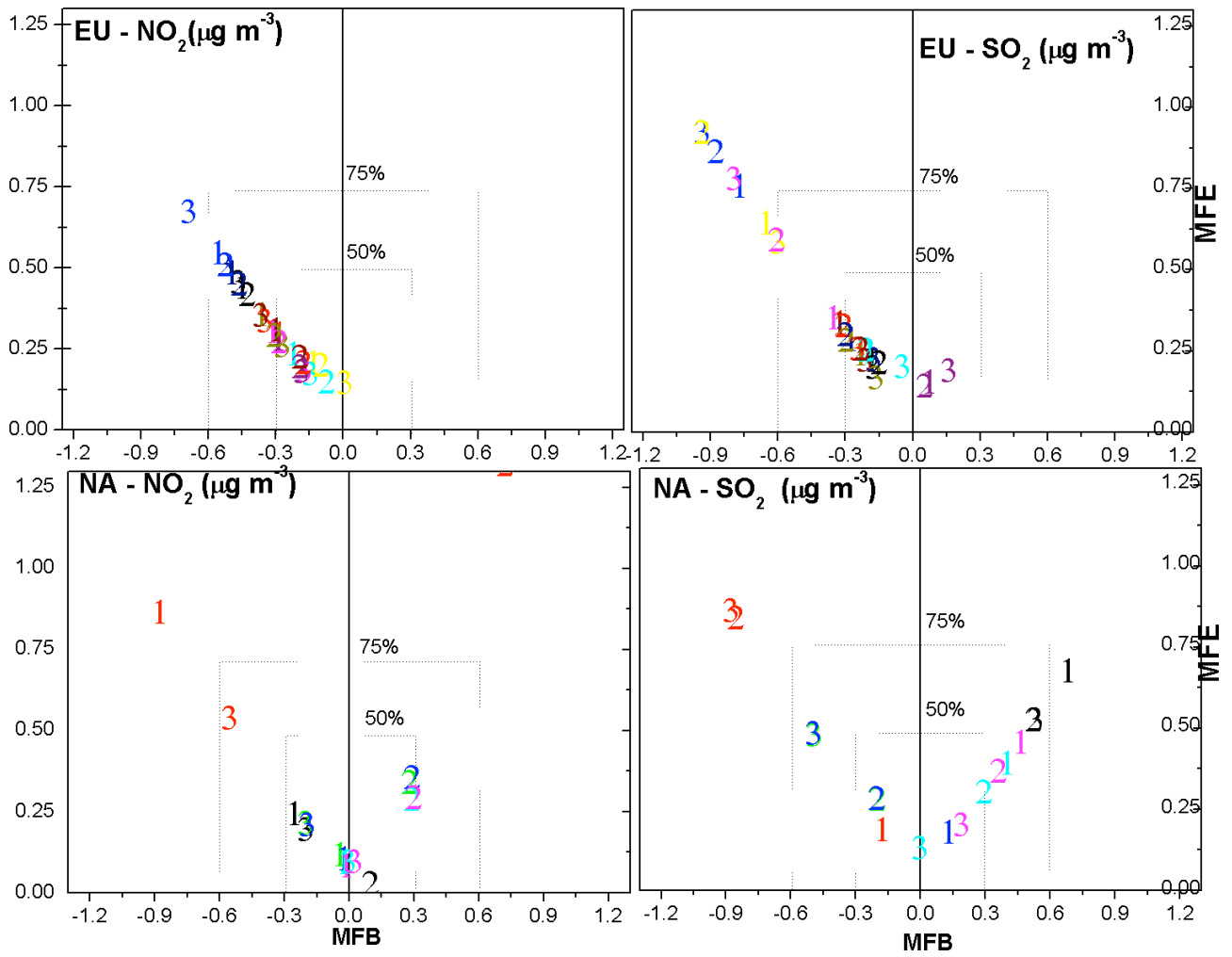
Figure 7.

PM10 Accumulated emission 2006 (kg km-2)
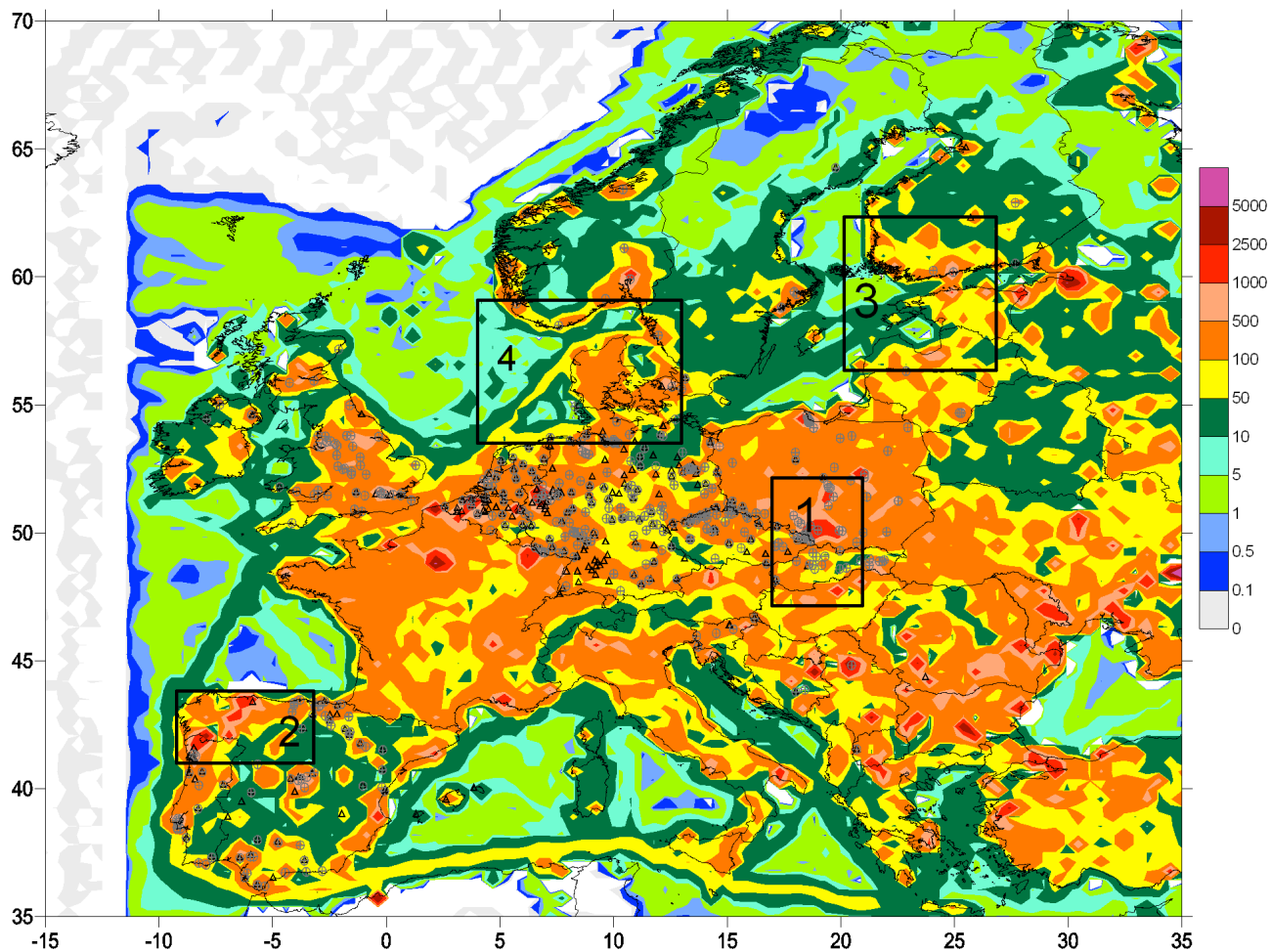
Figure 8a
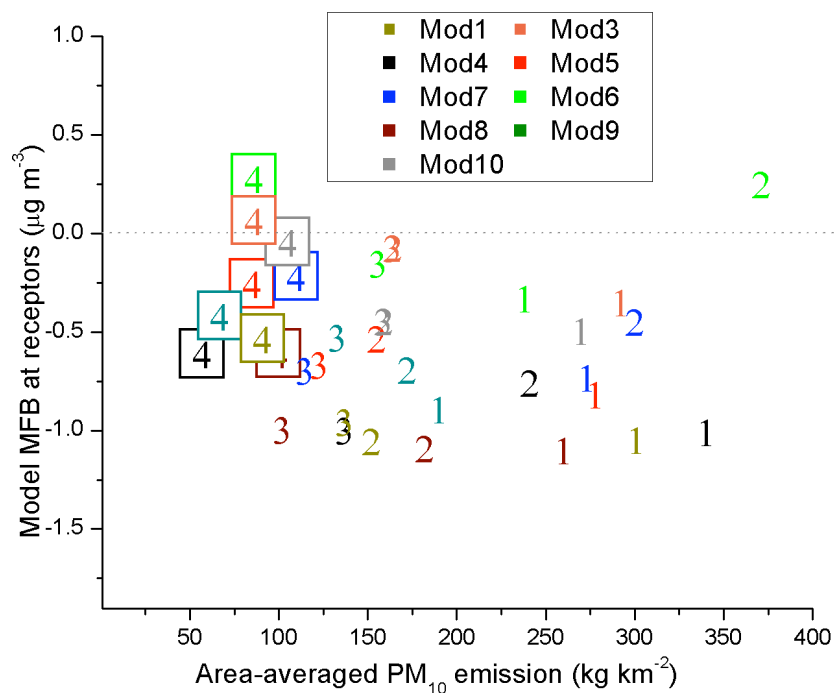
Figure 8b
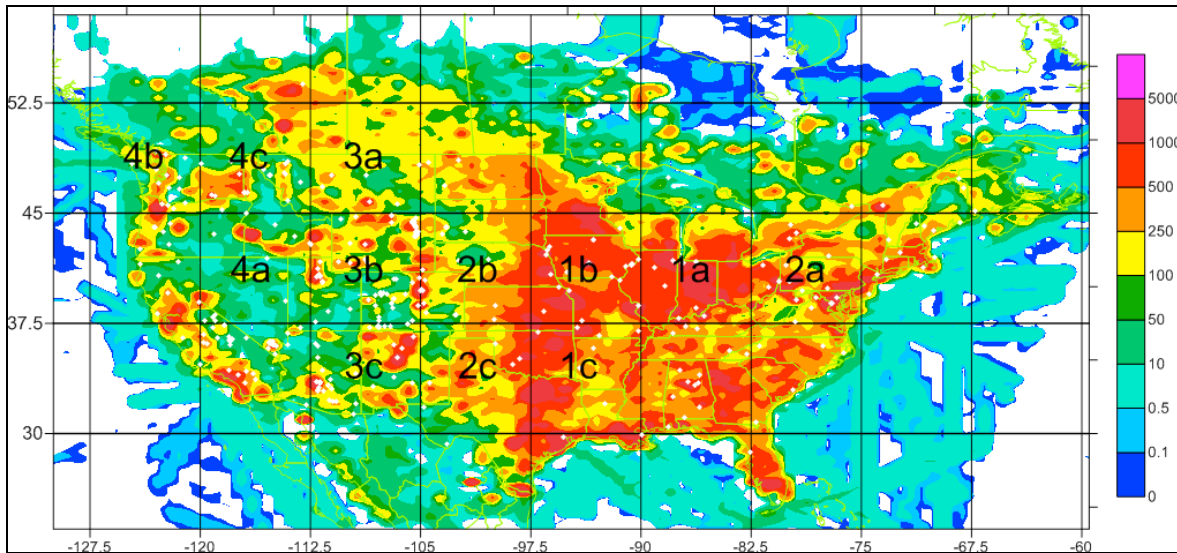
Figure 9a

Figure 9b

a)
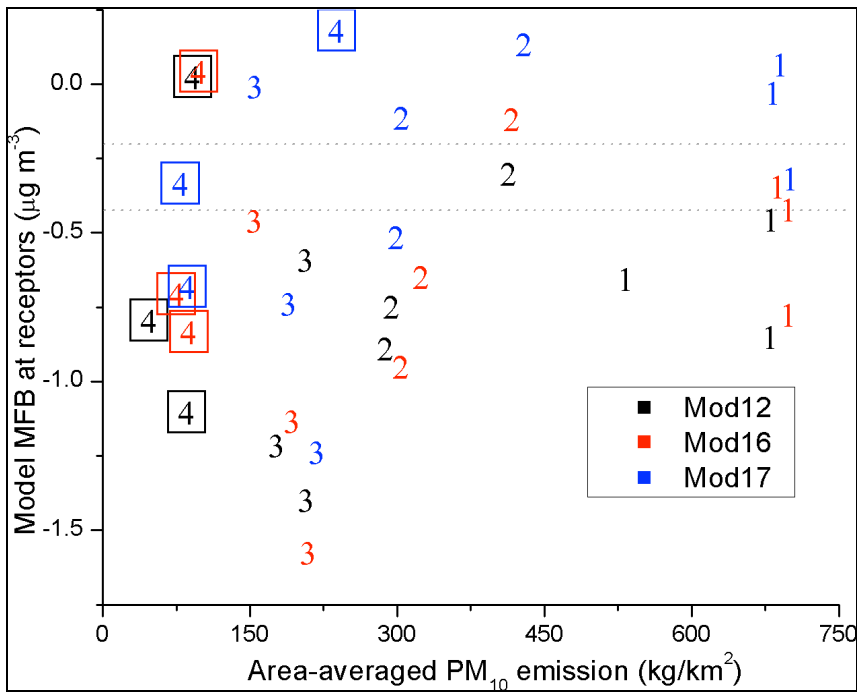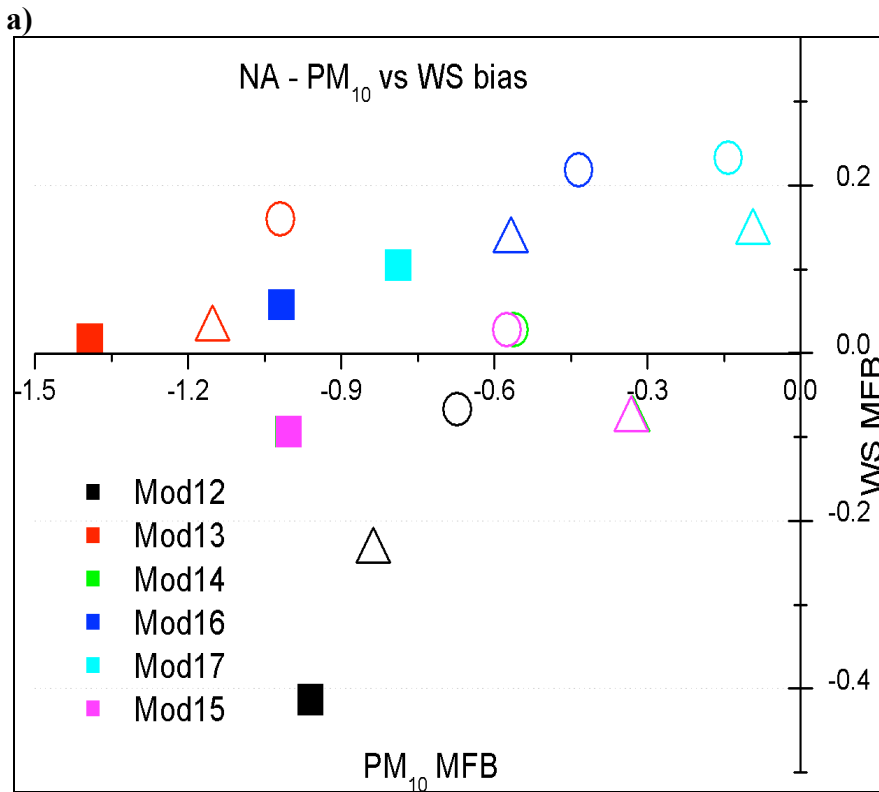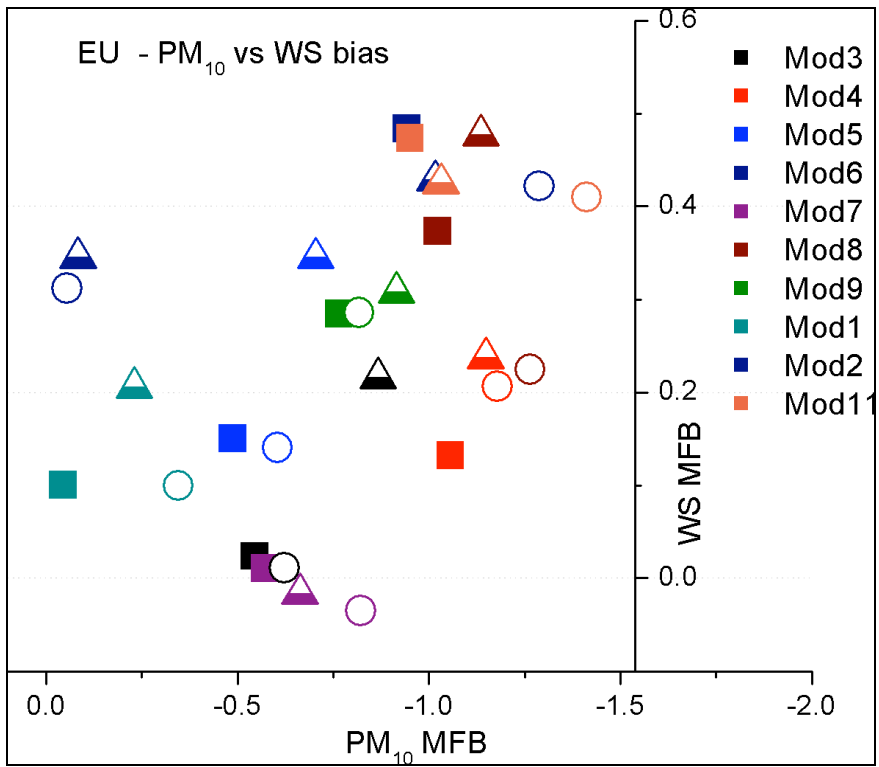
b)
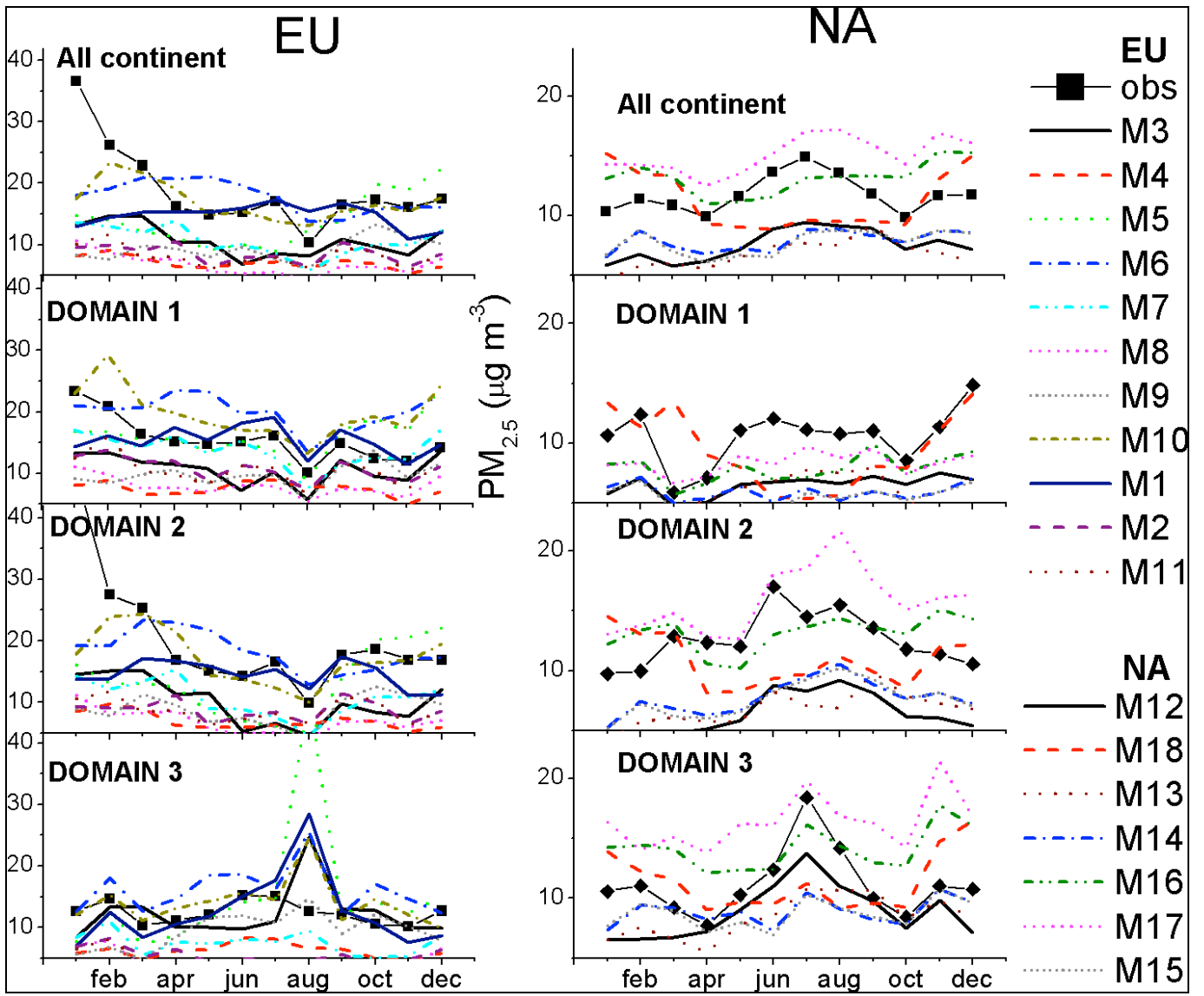
Figure 10

Figure 11
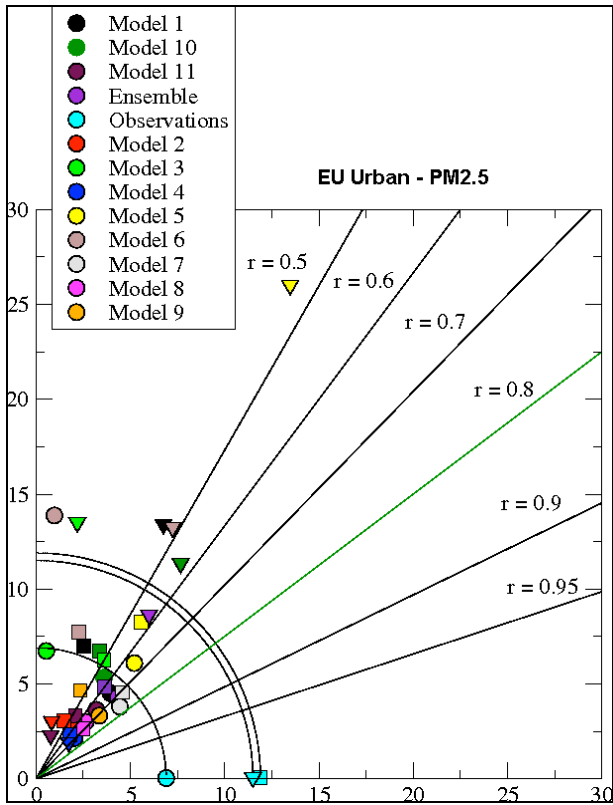
Figure 12a
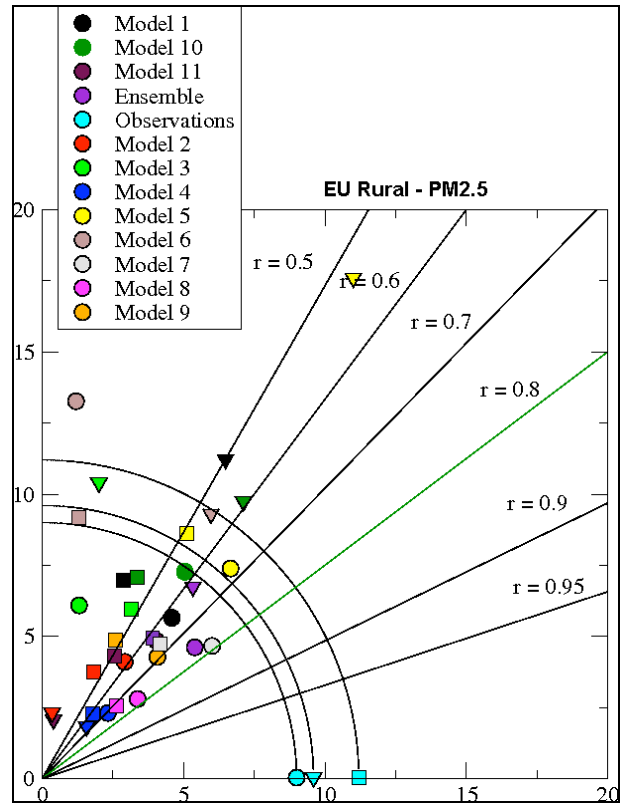
Figure 12b
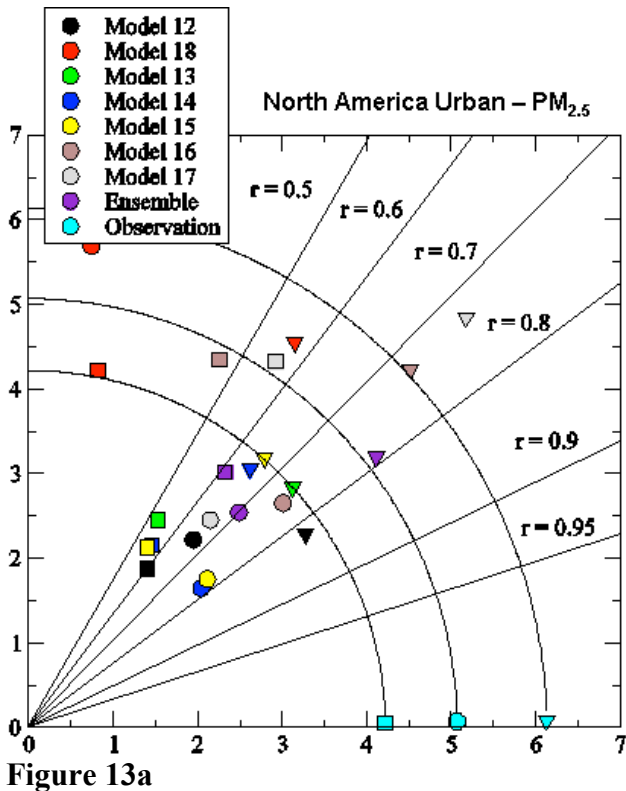
Figure 13a
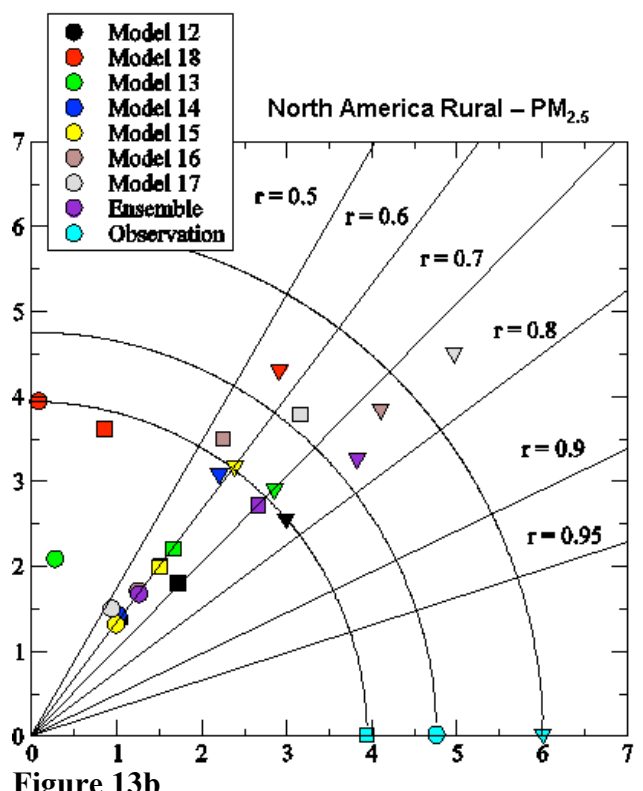
Figure 13b
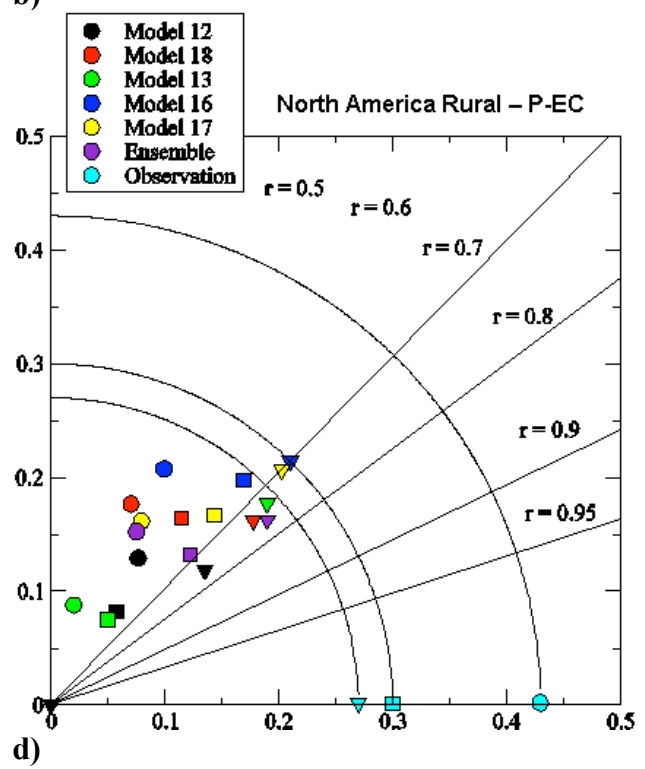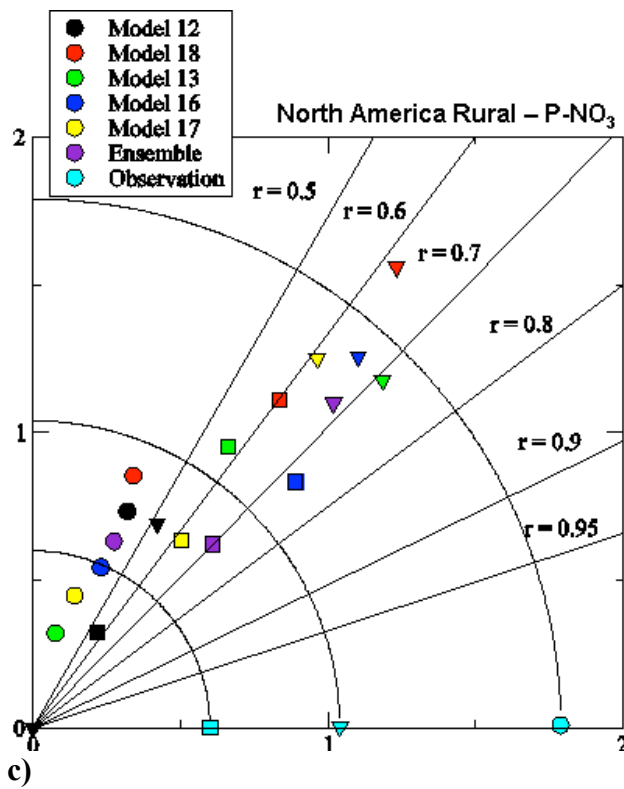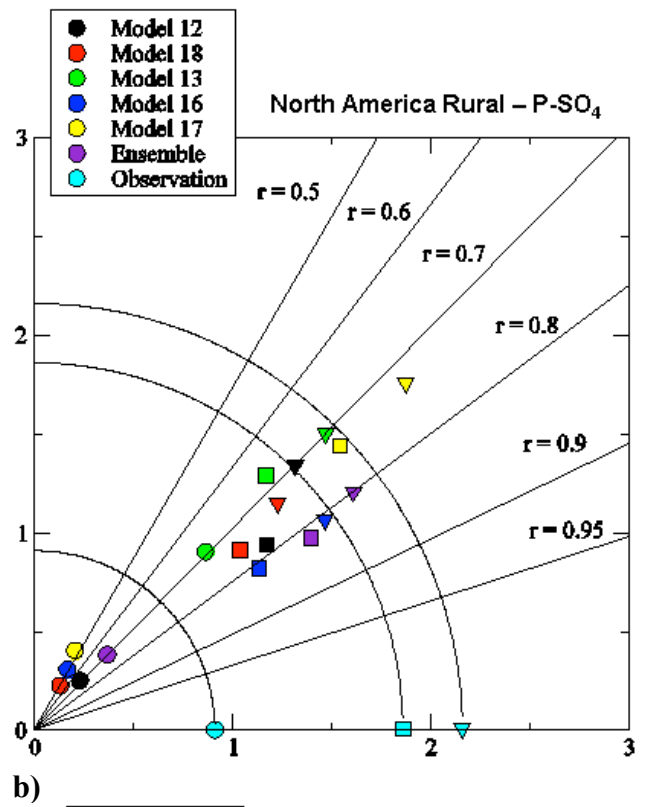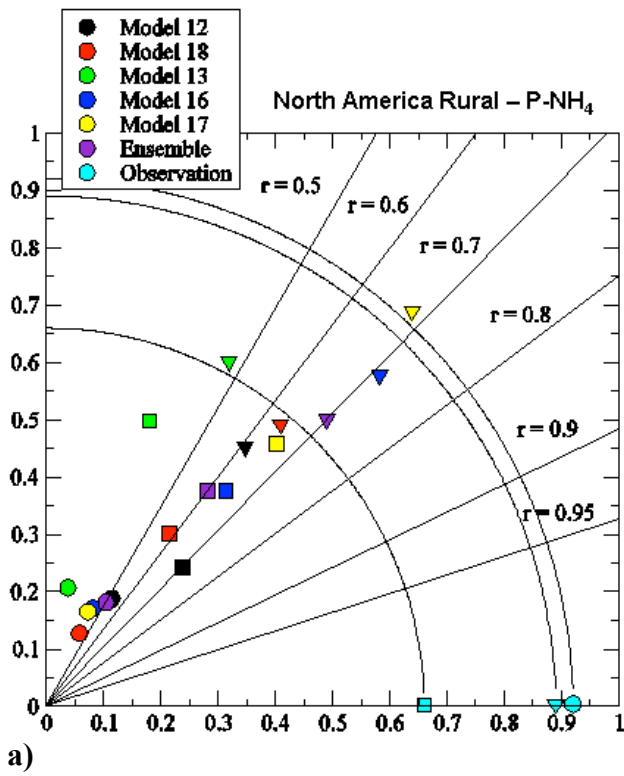
Figure 14

Figure 15

Figure 16